SCHOOL OF ADVANCED STUDIES OF THE ROMANIAN ACADEMY
DOCTORAL SCHOOL OF CHEMICAL SCIENCES
Petru Poni Institute of Macromolecular Chemistry
CHEMISTRY Field

COMPLEX POLYMERIC MATRICES WITH ANTIBACTERIAL INCLUSIONS

SUMMARY OF THE DOCTORAL THESIS

Ph.D. SUPERVISOR:
CS I DR. HABIL. LOREDANA ELENA NIȚĂ

Ph.D. STUDENT:
BIANCA-ELENA-BEATRICE CREȚU

2026

ROMANIAN ACADEMY

Petru Poni Institute of Macromolecular Chemistry

Mrs./Ms.....

We are pleased to announce that the public defense of the doctoral thesis **"*Complex polymeric matrices with antibacterial inclusions*"**, authored by **Bioeng. Bianca-Elena-Beatrice CREȚU**, will take place on **15 June 2026 at 11:00** in the Conference Room of the Petru Poni Institute of Macromolecular Chemistry, Iași, as part of the requirements for the conferment of the Doctor of Philosophy (Ph.D.) degree.

PRESIDENT: ***CS I Dr. Valeria HARABAGIU***

Petru Poni Institute of Macromolecular Chemistry, Iași

DOCTORAL SUPERVISOR: ***CS I Dr. Habil. Loredana Elena NIȚĂ***

Petru Poni Institute of Macromolecular Chemistry, Iași

REFEREES: ***Conf. Dr. Vera BĂLAN***

Grigore T. Popa University of Medicine and Pharmacy of Iași

Conf. Dr. Cătălina Anișoara PEPTU

Gheorghe Asachi Technical University of Iași

CS II Dr. Diana Elena CIOLACU

Petru Poni Institute of Macromolecular Chemistry, Iași

In accordance with the Regulations concerning the organization and conduct of doctoral studies for the award of scientific degrees within the Romanian Academy, we hereby submit the abstract of the doctoral thesis and kindly request that you communicate your evaluations and observations. We also take this opportunity to invite you to attend the public defense of the doctoral thesis.

Acknowledgements

The completion of this doctoral thesis is the result of an academic and professional journey supported by the trust, encouragement, and generosity of many individuals, to whom I would like to express my sincere gratitude.

First and foremost, I would like to thank my doctoral supervisor, ***CS I Dr. Habil. Loredana Elena Niță****, for her dedicated guidance, patience, professionalism, and confidence throughout my doctoral studies. Her advice, experience, and support have played an essential role in my development as a researcher and in the completion of this work.*

I would also like to express my gratitude and appreciation to ***CS I Dr. Valeria Harabagiu****,* ***Conf. Dr. Vera Bălan****,* ***Conf. Dr. Cătălina Anișoara Peptu****, and* ***CS II Dr. Diana Elena Ciolacu****, who honored me by accepting to serve on my doctoral examination committee as chair and reviewers. I am grateful for their willingness to evaluate this thesis, for the time they devoted to it, and for their valuable comments and recommendations, which have contributed significantly to improving this work.*

I would also like to thank the members of my doctoral advisory and academic integrity committee, ***CS I Dr. Aurica P. Chiriac****,* ***CS I Dr. Maria Bercea****,* ***CS III Dr. Alina Gabriela Rusu****, and* ***Conf. Dr. Gianina Dodi****, for their constant support throughout my doctoral studies, for their constructive suggestions, and for their significant contribution to my scientific development.*

My sincere appreciation goes to my research colleagues, ***Dr. Alexandra Vieru****,* ***Dr. Alina Ghilan****,* ***Dr. Isabella Nacu****, and* ***Ph.D. Student Alexandru-Mihail Șerban****, with whom I have shared challenges, achievements, and numerous professional experiences. Their teamwork, scientific discussions, and continuous support over the years have made this journey both easier and more rewarding.*

I would like to thank all my colleagues at the Petru Poni Institute of Macromolecular Chemistry for providing a stimulating academic environment and for their support and collaboration, which contributed to the completion of this doctoral thesis.

I am grateful to ***Dr. Antonella Caterina Boccia*** *for her support and guidance during my research internship at the Giulio Natta Institute of Chemical Sciences and Technologies in Milan, Italy.*

My appreciation also extends to my former colleagues and collaborators, ***Dr. Florina-Daniela Cojocaru****,* ***Dr. Ioannis Gardikiotis****,* ***Dr. Vlad-Constantin Ursachi****, and* ***Dr. Cosmin-Teodor Mihai****, who contributed to my professional and personal development and from whom I have learned a great deal.*

I would also like to thank my current colleagues and supervisors from the Research and Development Center – Pharmaceutical Development Activity, Antibiotice S.A., namely ***Dr. Iolanda Fusteș-Dămoc****,* ***Dr. Oana-Teodora Afloarea****,* ***Dr. Gabriela Buema****, and* ***Dr. Petronela Horlescu****, for their understanding and encouragement during the final months of this work.*

I am deeply grateful to my friends, especially ***Bioeng. Elena Dodițe****, for their constant encouragement and for providing moments of balance and joy during the demanding periods of this journey.*

Most importantly, I would like to thank my family for their unconditional support, understanding, trust, and love throughout every stage of my life. Without their encouragement, this journey would not have been possible.

I gratefully acknowledge the financial support provided by the Romanian Academy and the COTERAN and HYTECHSKIN projects throughout my doctoral studies.

I dedicate this thesis to my parents, to whom I owe the values that have shaped me, the strength to persevere, and the confidence to pursue my dreams. I thank them for all their sacrifices, for their unconditional love, and for always being by my side. This achievement belongs, to a great extent, to them as well.

Bianca-Elena-Beatrice Crețu

Iași, 2026

TABLE OF CONTENTS THESIS/SUMMARY

LIST OF ABBREVIATIONS

AFM – Atomic force microscopy

Amx – Amoxicillin

ATP – Adenosine triphosphate

α-Tcp – α-Tocopherol

B. cereus – Bacillus cereus

C. albicans – Candida albicans

CMC – Carboxymethyl chitosan

DLS – Dynamic light scattering

DNA – Deoxyribonucleic acid

DPPH – 2,2-diphenyl-1-picrylhydrazyl

DTG – Derivative thermogravimetry

EB – Ethylene brasylate

EE – Encapsulation efficiency

E. coli – Escherichia coli

E. faecalis – Enterococcus faecalis

ELISA – Enzyme-linked immunosorbent assay

FTIR – Fourier transform infrared spectroscopy

GPC – Gel permeation chromatography

H. influenzae – Haemophilus influenzae

IL–8 – Interleukin–8

K. pneumoniae – Klebsiella pneumoniae

MBC – Minimum bactericidal concentration

MIC – Minimum inhibitory concentration

MRSA – Methicillin-resistant *Staphylococcus aureus*

MSSA – Methicillin-sensitive *Staphylococcus aureus*

MTT – 3-(4,5-dimethylthiazol-2-yl)-2,5-diphenyltetrazolium bromide

NMR – Nuclear magnetic resonance

NRF – Norfloxacin

PAA – Poly(acrylic acid)

PAM – Poly(acrylamide)

P. aeruginosa – Pseudomonas aeruginosa

PEG – Poly(ethylene glycol)

PHA – Polyhydroxyalkanoates

PHB – Poly(3-hydroxybutyrate)

PHEMA – Poly(2-hydroxyethyl methacrylate)

PEB – Poly(ethylene brasylate)

PEBSA – Poly(ethylene brasylate-co-squaric acid)

PTSA – p-Toluenesulfonic acid

PVA – Poly(vinyl alcohol)

PVP – Poly(N-vinyl-2-pyrrolidone)

RNA – Ribonucleic acid

ROS – Reactive oxygen species

SA – Squaric acid

SEM – Scanning electron microscopy

S_{ent} – Surface entropy

S_q – Root mean square roughness

S. aureus – Staphylococcus aureus

S. pneumoniae – Streptococcus pneumoniae

S_{tdi} – Surface texture direction index

STEM – Scanning transmission electron microscopy

T_{10}, T_{20} – Temperatures corresponding to 10% and 20% mass loss, respectively

TBD – 1,5,7-Triazabicyclo[4.4.0]dec-5-ene

TG – Thermogravimetry

Thy – Thymol

T_{onset} – Onset degradation temperature

T_{peak} – Temperature at maximum degradation rate

TSP – Sodium 3-(trimethylsilyl)-2,2,3,3-tetradeuteropropionate

W – Mass loss at the end of the decomposition stage

XRD – X-ray diffraction

INTRODUCTION

Bacterial infections are a common complication associated with skin wounds [1], contributing to further delays in the healing process and even to local tissue necrosis [2]. Wound management aims to eliminate all factors that may hinder healing while creating and maintaining optimal conditions to support this process [3]. Materials such as cotton and gauze are widely used as wound dressings due to their ability to isolate the wound from the external environment; however, they do not possess antibacterial properties and are not suitable for all types of lesions. Furthermore, studies have demonstrated that wound healing occurs approximately twice as fast in moist environments compared to dry ones, leading to a progressive transition from traditional cotton and gauze dressings to hydroactive dressings [4]. The successful use of hydrogel dressings in the care and treatment of skin wounds is attributed to their structural and compositional similarity to the body's soft tissues [5]. Hydrogels are capable of absorbing and maintaining an optimal level of wound exudate at the wound surface while ensuring the gas exchange required for cell proliferation [6].

Poly(vinyl alcohol) (PVA) is one of the most widely used water-soluble synthetic polymers for the preparation of hydrogels through successive freeze–thaw cycles, owing to its ability to undergo physical crosslinking. This approach eliminates the need for chemical crosslinking agents, thereby reducing toxicological concerns and providing hydrogels with a high degree of purity [7]. The resulting hydrogels exhibit remarkable properties, including excellent biocompatibility, suitable elasticity, and high water absorption and retention capacities [8]. However, two major challenges limiting the use of PVA-based hydrogels as biomaterials have been identified in the literature: their lack of intrinsic bioactivity and the difficulty of efficiently incorporating predominantly hydrophobic antibacterial agents into the polymer matrix.

The encapsulation of therapeutic agents within a polymeric matrix offers multiple advantages, including protection against moisture, free radicals, and oxygen; prevention of undesirable chemical reactions between active species; modification of density, color, or photosensitivity; and enhanced system stability [9]. From an application-oriented perspective, this technology enables more efficient preservation and easier handling of active compounds while also promoting their sustained release. Consequently, it represents a promising strategy for controlling the skin regeneration process and reducing microbial contamination, both of

which are essential factors in facilitating wound healing.

Based on these considerations, the overall objective of the doctoral thesis entitled **"Complex polymeric matrices with antibacterial inclusions"** was to:

> ***Design, synthesis, and characterization of novel polymeric structures with a tunable hydrophilic/hydrophobic ratio, based on synthetic and/or natural polymers, capable of improving the solubility, stability, and bioavailability of hydrophobic antibacterial agents for cutaneous applications.***

The **motivation** for the research direction addressed in the present doctoral thesis is based on the understanding of the mechanisms of formation of three-dimensional structures and the optimization of the characteristics of multicomponent hydrogels for their use as supporting matrices for antibacterial agents with low solubility in common solvents, but with significant therapeutic value.

The following **specific objectives** are considered as possible approaches: (**O1**) the synthesis of new homo- and copolymers based on biodegradable polyesters derived from renewable resources, with applications in the controlled release of hydrophobic antibacterial agents; (**O2**) the preparation of polymeric nanoparticles loaded with a broad-spectrum antibacterial antibiotic; (**O3**) the development of multicomponent hydrogels with (nano)antibacterial and antioxidant inclusions using the freeze–thaw technique; (**O4**) physicochemical characterization and selection of optimal formulations for (**O5**) evaluation of antibacterial and antioxidant activity, *in vitro* cytotoxicity, and *in vivo* studies regarding their applicability in the development of wound dressings for the treatment of skin wounds.

The doctoral thesis comprises six chapters, structured into two distinct parts, as presented below.

Part I includes **Chapter I**, which is dedicated to the presentation of relevant literature data on the studied topic: theoretical concepts regarding the definition and classification of hydrogels, the current state of research in the field of antibacterial hydrogels based on synthetic and/or natural polymers, their properties, as well as a synthesis of the main physicochemical characterization methods, together with *in vitro* and *in vivo* studies used to evaluate their applicative potential in tissue engineering and regenerative medicine.

Part II is structured into five chapters (Chapters II–VI) and presents the original contributions regarding the development, physicochemical characterization, and *in vitro*/*in vivo* evaluation of the obtained antibacterial multicomponent hydrogels.

Chapter II describes the experimental section, which includes the materials, equipment, and analytical methods used within the doctoral study.

Chapter III presents a series of polymeric hydrogel matrices based on PVA and poly(ethylene brassilate) (PEB), evaluating their potential to incorporate drug-loaded nanoparticles and to be used as controlled drug delivery systems for active substances. The hydrogels were prepared in three stages: (1) synthesis of the PEB homopolymer via ring-opening polymerization of ethylene brassilate (EB) in bulk and in solution (using 1,4-dioxane as solvent), in the presence of 1-hexanol as initiator and two organic catalysts, *p*-toluenesulfonic acid (PTSA) and 1,5,7-triazabicyclo[4.4.0]dec-5-ene (TBD); (2) preparation of PEB-based nanoparticles by the precipitation method, with norfloxacin (NRF) being *in situ* incorporated into the homopolymeric matrix; (3) preparation of PVA-based hydrogels loaded with homopolymer–drug nanoparticle systems using the freeze–thaw technique. The formation of the homopolymer was confirmed by structural analyses (FTIR, ^{1}H NMR, XRD). The obtained nanoparticles exhibited a predominantly spherical morphology and a core–shell structure. The results demonstrated the potential of the hydrogels to provide a sustained release profile of NRF under *in vitro* conditions over 48 h.

Chapter IV presents original results regarding the development and characterization of multicomponent hydrogels with antibacterial and antioxidant inclusions based on PVA, poly(ethylene brassilate-co-squaric acid) (PEBSA), thymol (Thy), and α-tocopherol (α-Tcp), as well as the investigation of the synergistic potential between these two bioactive compounds. The study aimed to evaluate how the presence of the amphiphilic copolymer PEBSA – used to facilitate the encapsulation of hydrophobic bioactive compounds within the network – influences the properties of the polymeric matrices. The obtained results showed that PVA_PEBSA systems allow control over surface properties and porosity by adjusting the molar ratio of the EB:squaric acid (SA) comonomers in the PEBSA composition. Cumulative release profiles of Thy_α-Tcp confirmed the ability of the PVA_PEBSA system to incorporate and provide controlled and sustained release of bioactive compounds under simulated physiological conditions. The systems exhibited bacteriostatic activity against the growth of *Staphylococcus*

aureus (*S. aureus*), *Escherichia coli* (*E. coli*), and *Candida albicans* (*C. albicans*). The cumulative antioxidant activity of Thy and α-Tcp in association with PEBSA produced a notable synergistic effect. *In vitro* cytotoxicity tests on the BALB/3T3 clone A31 cell line indicated the absence of cytotoxicity of the antibacterial materials, with cell viability values higher than 90% after 72 h of contact. The *in vivo* biocompatibility assessment study through subcutaneous implantation in Wistar rats confirmed the biocompatibility of the tested materials, their integration with the host tissue, and the absence of an inflammatory response. The antibacterial hydrogels significantly contributed to the reduction of wound size in Wistar rats. At 20 days after the onset of the experiment, almost complete tissue regeneration was observed.

Chapter V describes the preparation and characterization of antibacterial hybrid double-network hydrogels obtained by integrating natural polymers (dextran and xanthan gum) into PVA_PEBSA polymer matrices. The introduction of these two polysaccharides aimed to develop hybrid materials with advanced properties for regenerative medicine applications, such as increased bioadhesiveness, controlled morphology, high swelling capacity, and effective conformability to wound geometry. At the same time, the study considered achieving controlled biodegradability in a biological environment while maintaining biocompatibility. This chapter presents the development and characterization of two variants of multicomponent hybrid antibacterial hydrogels: (1) hybrid antibacterial hydrogels based on PVA, PEBSA, dextran, and amoxicillin (Amx), and (2) hybrid antibacterial hydrogels based on PVA, PEBSA, xanthan gum, and Amx. The systems were characterized structurally, morphologically, and in terms of their capacity to retain simulated biological fluids. In addition, *in vitro* enzymatic degradation studies were performed, along with quantitative analysis of the active pharmaceutical ingredient released via ^{1}H NMR, evaluation of antibacterial activity against *Staphylococcus aureus*, *Escherichia coli*, *Klebsiella pneumoniae* (*K. pneumoniae*), *Enterococcus faecalis* (*E. faecalis*), and *in vitro* studies on normal human dermal fibroblasts. The correlation of the obtained results supports the use of antibacterial hybrid hydrogels as efficient controlled drug delivery systems in tissue engineering applications, ensuring prolonged availability of the bioactive substance over the long term.

The final chapter of the doctoral thesis, **Chapter VI**, presents the conclusions referring to the most important experimentally obtained results, as well as future research directions.

The doctoral thesis is structured as follows:

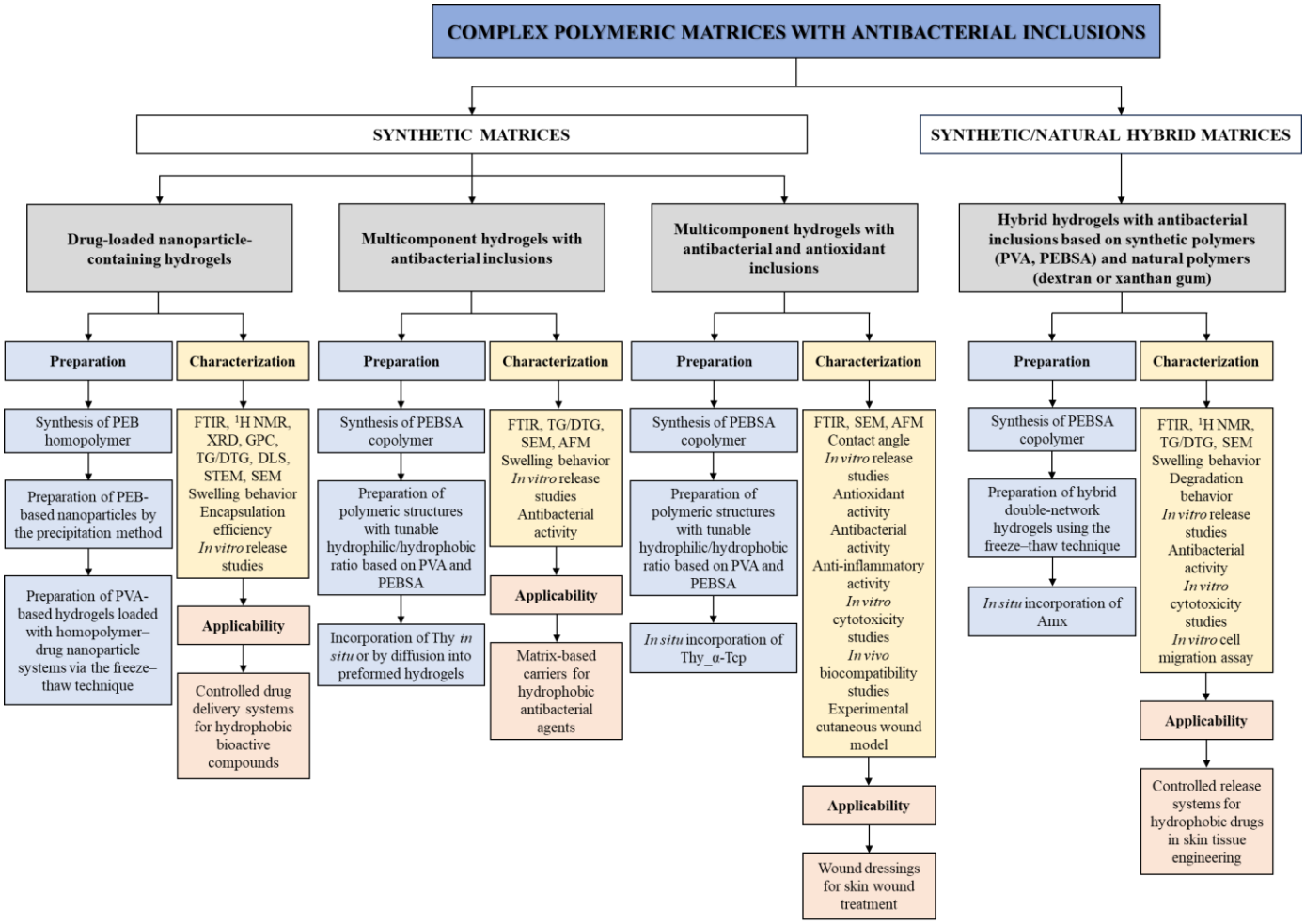

The doctoral thesis comprises 179 pages and is divided into six chapters, including 34 tables, 89 figures, 14 equations, and 248 bibliographic references. The following appendices are included at the end of the thesis:

Appendix 1 – Dissemination of results and scientific activity

Appendix 2 – Scientific articles

The original results obtained within the doctoral thesis constitute the subject of **five scientific articles** published in ISI-indexed journals (cumulative impact factor = 20.3), **three oral communications**, and **three posters** presented at international scientific conferences. *The related scientific activity associated* with the topic of the doctoral thesis resulted in three scientific articles published in ISI-indexed journals (cumulative impact factor = 15), **one book** currently in press, **one patent application**, **two oral communications**, and **five posters** presented at international scientific conferences.

PART II. ORIGINAL CONTRIBUTIONS

CHAPTER III. POLY(VINYL ALCOHOL)-BASED HYDROGELS CONTAINING WITH DRUG-LOADED NANOPARTICLES

III.1. Research background

Growing global concerns regarding the environmental impact of conventional petroleum-derived polyolefinic materials have led to intensified efforts toward the development of sustainable alternatives, such as polymers obtained from renewable resources. Compared to traditional polymers, their main advantage lies in the renewability of the raw materials [151].

Among all polymers derived from renewable resources, aliphatic polyesters have attracted considerable interest, being extensively studied as biodegradable and biocompatible materials for applications in the medical field and packaging materials [152]. A relevant example is PEB, a biodegradable aliphatic homopolymer, which makes it suitable for applications where sustainability is a priority or for biomedical uses. The structure of its repeating unit, featuring a long apolar chain between ester linkages, confers pronounced hydrophobicity, low water uptake, and higher resistance to hydrolytic degradation compared to polyesters such as poly(lactic acid), which have a more polar structure. At the same time, the biocompatibility of PEB makes it a promising material for biomedical applications, such as the development of carriers for hydrophobic bioactive compounds [38–41].

PEB is synthesized via the ring-opening polymerization of EB, a cyclic lactone containing two ester groups. EB is commercially produced through the condensation reaction of ethylene glycol with 1,13-tridecanedioic acid [37], which is derived from castor oil – an economically accessible renewable resource [153]. The polymerization of EB has been carried out at laboratory scale using enzymatic [154], organometallic [37], or organic catalysts [155]. In contrast to metal-based catalysts, organic catalysts offer significant advantages, including reduced toxicity, lower environmental impact, lower cost compared to enzymatic catalysts, and good biocompatibility [156].

III.2. Specific scientific objectives:

- Synthesis and physicochemical characterization of the PEB homopolymer;

- Preparation of PEB-based nanoparticles loaded with NRF, a broad-spectrum antibacterial antibiotic, and their characterization in terms of size, physical stability, encapsulation efficiency, and morphology;
- Preparation of PVA-based hydrogels loaded with drug-carrying nanoparticles using the freeze–thaw technique, and characterization of the systems to obtain information regarding chemical composition, morphology, determination of simulated biological fluid retention capacity, and quantitative analysis of the released active compound.

III.3. Synthesis and characterization of poly(ethylene brasylate) homopolymer

The study focused on the development of sustainable methods for the synthesis of the PEB homopolymer, with an emphasis on reaction efficiency and the minimization of environmental impact. From the perspective of green chemistry, one of the current challenges in the synthesis of aliphatic PEB polyesters is the use of more environmentally friendly solvents. In order to replace traditional solvents such as toluene, chloroform, or diethyl ether, this study explores an alternative strategy. The novelty of the research lies in the solution-based synthesis of EB in a homogeneous system using 1,4-dioxane as solvent.

1,4-Dioxane is an organic solvent with a low dielectric constant, which reduces significant charge separation or dissociation of the formed catalytic complex. In this synthesis, low-molecular-weight alcohols are commonly used to control the molecular weight of polyesters [37,157]. In this case, 1-hexanol was added to the reaction mixture. In contrast to Pascual et al. [155,158], considered pioneers in the use of organic catalysts for EB polymerization, who purified the crude homopolymer by dissolution in a 10% dichloromethane solution and precipitation with cold diethyl ether (1:5), the present study proposes an alternative purification method based on repeated wash–sedimentation cycles in cold distilled water (2–8 °C).

III.3.1. Synthesis procedure

The PEB homopolymer was synthesized via ring-opening polymerization of EB in bulk and in solution (using 1,4-dioxane as solvent), in the presence of 1-hexanol as initiator and two organic catalysts, PTSA and TBD (**Figure 3.1.**). The reactions were carried out under a nitrogen atmosphere at a constant temperature of 105 °C, with magnetic stirring at 250 rpm for 24 h. A typical experiment for the **PEB_{100}_TBD** variant (**Table 3.1.**) involved the use of 11.52 mL EB (44.38 mmol, 100 equiv.), 0.0617 g TBD (0.4438 mmol, 1 equiv.), 0.6 mL 1-hexanol, and 48

mL 1,4-dioxane. To evaluate monomer conversion, aliquots were collected at different time intervals and precipitated in a distilled water–acetone mixture (2:1) at 2–8 °C. The precipitate was filtered and dried at room temperature, and conversion was determined using a gravimetric method. Purification of the final reaction mixture was performed through repeated wash–sedimentation cycles in distilled water. The resulting product was frozen in liquid nitrogen and lyophilized for 24 h at −55 °C (Alpha 1-2LD Plus, Martin Christ, Germany).

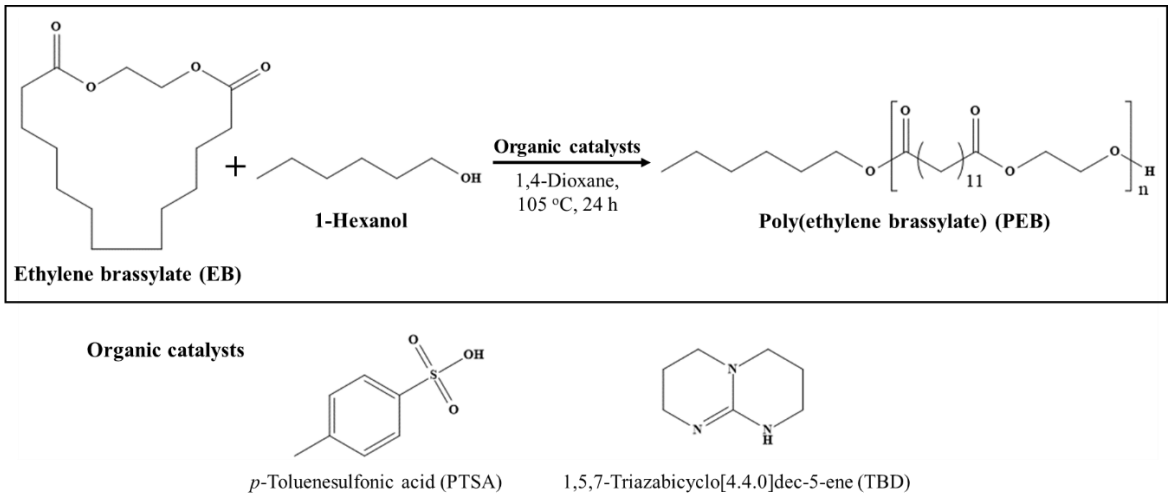

Figure 3.1. Schematic representation of the synthesis of the PEB homopolymer.

The experimental plan includes:

(1) the study of the influence of the *type of organic catalyst* on *monomer conversion into homopolymer*;

(2) the study of the influence of the *solvent* on *molecular weight distribution*;

(3) the study of the influence of the *monomer-to-catalyst ratio* on *monomer conversion into homopolymer* and *molecular weight distribution*.

The obtained experimental data are presented in **Table 3.1.**

Table 3.1. Influence of reaction parameters on monomer conversion to homopolymer.

Sample code	Catalyst	EB:Catalyst (equiv.)	Conversion (%)	Monomer (mol L^{-1})
PEB_{50}_PTSA	PTSA	50:1	70.83	0.26
PEB_{50}_TBD	TBD	50:1	82.75	0.15
PEB_{100}_TBD	TBD	100:1	78.5	0.22
PEB_{100}_TBD without 1-Hexanol	TBD	100:1	77.83	0.20
PEB_{150}_TBD	TBD	150:1	76.66	0.22

Figure 3.3. shows the conversion profiles for the solution polymerization of EB at different monomer concentrations. Experimentally, it was observed that the monomer polymerization rate is accelerated in the presence of TBD, whereas in the presence of PTSA the process becomes significantly more complex.

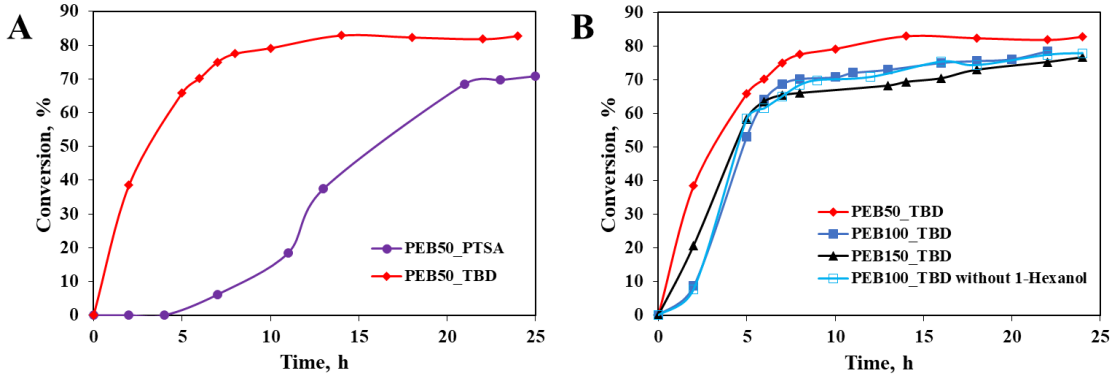

Figure 3.3. Conversion profiles of EB polymerization at 105 °C, initiated with 1-hexanol and catalyzed by (**A**) PTSA or (**B**) TBD in solution, for different monomer concentrations.

Surprisingly, a conversion of 77% was obtained even in the absence of 1-hexanol, a phenomenon accompanied by an increase in molecular weight. More specifically, a weight-average molecular weight of 2031 g/mol was achieved without the use of the initiator, compared to 1463 g/mol when it was present. These results confirm that TBD not only participates in the polymerization process as a catalyst but can also act as an initiator, influencing both the reaction kinetics and the molecular weight distribution [158]. This behavior highlights the dual role of the TBD catalyst, emphasizing its importance in optimizing the polymerization reaction.

The spectroscopic analyses performed (FTIR and ^{1}H NMR) confirmed the chemical structure of the synthesized homopolymers. The crystalline fraction of the homopolymer was determined by integrating the area under the crystalline peaks and the area corresponding to the amorphous phase in the diffractogram, using OriginPro 8.5 software, resulting in a crystallinity degree of approximately 57.2%. The average crystallite size of **PEB$_{50}$_TBD**, calculated using the Scherrer equation, was estimated at 25.3 nm. According to thermogravimetric data, the degradation process occurred in a single step, with a maximum thermal degradation temperature (T_{peak}) of approximately 454 °C and a residual mass of 1.16%. This result is in agreement with literature data [37,155].

III.4. PEB-based homopolymer–drug nanoparticle systems

The aim of the study was to obtain nanoparticulate carriers for hydrophobic drugs

based on the PEB homopolymer, designed for the encapsulation of NRF, in order to improve its solubility, stability, and bioavailability in biological environments.

III.4.1. Preparation of PEB-based nanoparticles loaded with NRF

PEB-based nanoparticles obtained via bulk polymerization (PM_{50}-NRF) and solution polymerization (**PS_{50}-NRF**, **PS_{100}-NRF**, **PS_{150}-NRF**) were prepared using the precipitation method, with NRF being *in situ* incorporated into the homopolymeric matrix (**Figure 3.7.**). Purification of the nanoparticles was carried out by dialysis against double-distilled water for 48 h, with the water being replaced every 12 h.

Drug-free nanoparticles (**PM_{50}**, **PS_{50}**, **PS_{100}**, **PS_{150}**) were prepared under similar conditions and used as a reference in subsequent analyses.

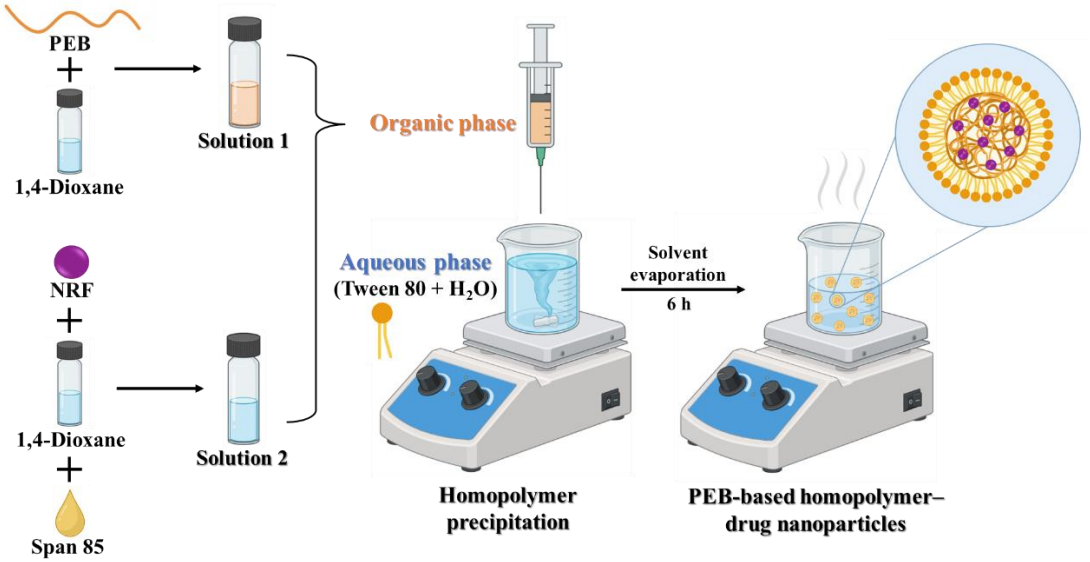

Figure 3.7. Schematic representation of the preparation steps of PEB-based homopolymer–drug nanoparticles.

DLS investigations showed that the hydrodynamic diameter of the nanoparticles depends on the molecular weight distribution of the corresponding PEB homopolymers, with sizes ranging between 190.6 and 290.7 nm. Moreover, all polydispersity index values were below 0.5, indicating a good degree of nanoparticle homogeneity. **Figure 3.9. A** presents STEM images of PEB_{50}_TBD-based nanoparticles (**PS_{50}**), highlighting their assembly into quasi-spherical nanoscale structures. The **PS_{50}-NRF** nanoparticles exhibit a uniform spherical morphology with a core–shell structure (**Figure 3.9. B**). Measurements performed using ImageJ software showed that NRF incorporation reduces the average nanoparticle diameter compared

to unloaded particles, as a result of intermolecular physical interactions between the homopolymer and the drug, a hypothesis also supported by DLS analysis.

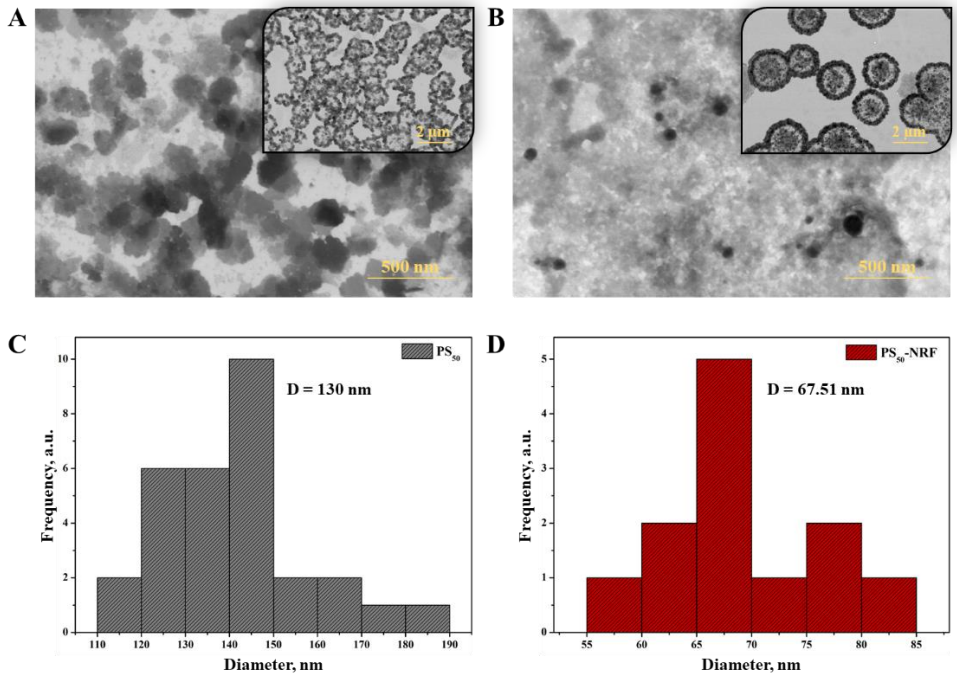

Figure 3.9. STEM images and particle size distribution histograms of PS_{50} systems (**A** and **C**) and PS_{50}-NRF systems (**B** and **D**), respectively.

III.5. Preparation and characterization of PVA-based hydrogels loaded with drug-carrying nanoparticles

The aim of the research was the preparation and characterization of novel PVA-based hydrogels loaded with drug-carrying nanoparticles, with the objective of facilitating their handling and ensuring a sustained release profile of the active substance.

III.5.1. Preparation of PVA_PS_{50}-NRF-based hydrogels

The preparation of PVA-based hydrogels with different molecular weights (72,000 and 145,000 g/mol) loaded with PS_{50}-NRF nanoparticles was carried out in a stepwise manner. Initially, a 4% PVA solution was prepared by dissolving an appropriate amount of PVA in distilled water at a constant temperature of 90 °C, under magnetic stirring at 700 rpm for 2 h under the same conditions. PEB-based nanoparticles in solution (PS_{50}-NRF) were prepared according to the protocol described in subchapter *III.4.1. Preparation of PEB-based nanoparticles loaded with NRF*. Subsequently, the individually prepared solutions were mixed at PVA:PS_{50}-NRF volumetric ratios of 3:1, 2:1, and 1:1, respectively, and subjected to 3 freeze–

thaw cycles, consisting of 18 h at –20 °C followed by thawing for 8 h at room temperature. Twelve hydrogel formulations with different compositions were obtained, as shown in **Table 3.6.** The resulting hydrogels were frozen in liquid nitrogen, lyophilized for 24 h at –55 °C (Alpha 1-2LD Plus, Martin Christ, Germany), and stored in a desiccator at room temperature for further studies.

Table 3.6. Coding of PVA_PS_{50}-NRF-based systems.

Sample code*	PVA:PS_{50} volumetric ratio	Observations	Figures
PVA_{72000}_PS_{50}_3:1	3:1	Structured and homogeneous hydrogel	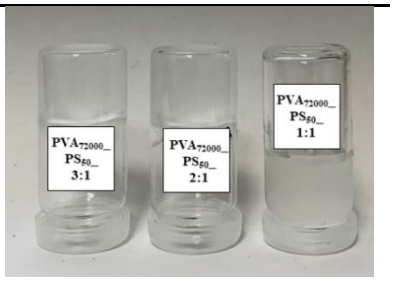
PVA_{72000}_PS_{50}_2:1	2:1	Structured and homogeneous hydrogel	
PVA_{72000}_PS_{50}_1:1	1:1	Inhomogeneous hydrogel with phase separation	
PVA_{72000}_PS_{50}-NRF_3:1	3:1	Structured and homogeneous hydrogel	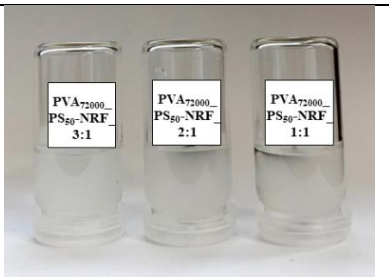
PVA_{72000}_PS_{50}-NRF_2:1	2:1	Inhomogeneous hydrogel with phase separation	
PVA_{72000}_PS_{50}-NRF_1:1	1:1	Inhomogeneous hydrogel with phase separation	
PVA_{145000}_PS_{50}_3:1	3:1	Compact and homogeneous hydrogel	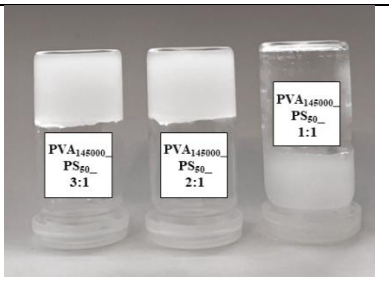
PVA_{145000}_PS_{50}_2:1	2:1	Compact and homogeneous hydrogel	
PVA_{145000}_PS_{50}_1:1	1:1	Compact and homogeneous hydrogel	
PVA_{145000}_PS_{50}-NRF_3:1	3:1	Compact and homogeneous hydrogel	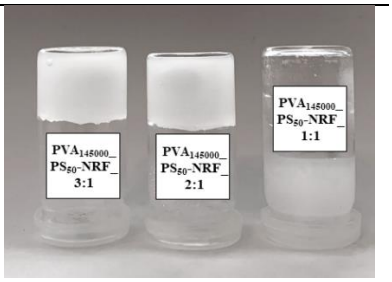
PVA_{145000}_PS_{50}-NRF_2:1	2:1	Compact and homogeneous hydrogel	
PVA_{145000}_PS_{50}-NRF_1:1	1:1	Compact and homogeneous hydrogel	

* 4% concentration for both PVA solutions

The observations revealed that PVA-based hydrogels with a molecular weight of 145,000 g/mol exhibit a compact and homogeneous structure. Due to these characteristics, these

hydrogel formulations were selected for characterization in subchapter *III.5.2. Characterization methods of PVA_PS$_{50}$-NRF-based hydrogels*. SEM images highlight that all samples possess a porous internal structure characterized by interconnected pores of variable size (**Figure 3.11.**).

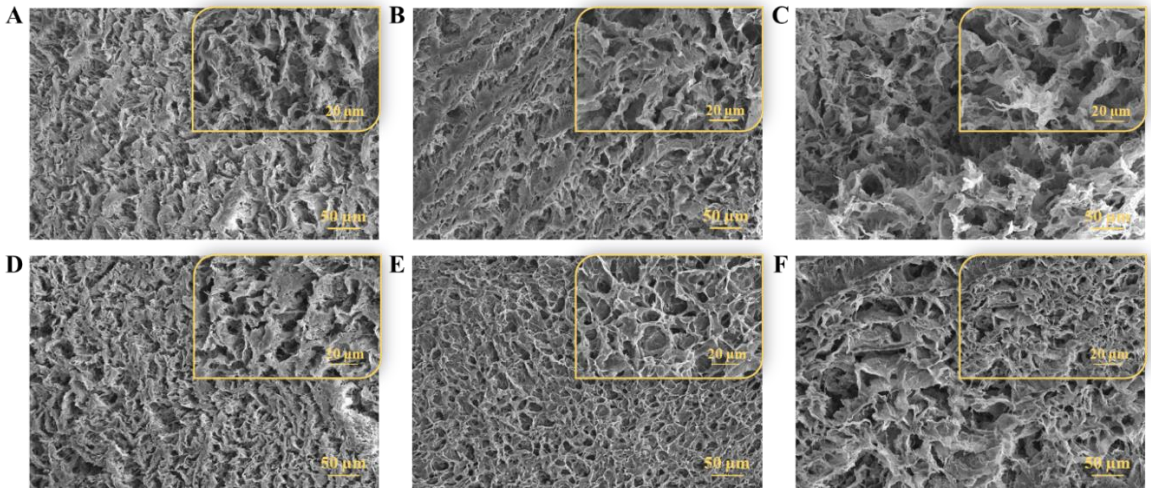

Figure 3.11. SEM images of the samples: (**A**) PVA$_{145000}$_PS$_{50}$_3:1, (**B**) PVA$_{145000}$_PS$_{50}$_2:1, (**C**) PVA$_{145000}$_PS$_{50}$_1:1, (**D**) PVA$_{145000}$_PS$_{50}$-NRF_3:1, (**E**) PVA$_{145000}$_PS$_{50}$-NRF_2:1, and (**F**) PVA$_{145000}$_PS$_{50}$-NRF_1:1.

The maximum amount of antibiotic released over a period of 48 h was 37.83% (**PVA$_{145000}$_PS$_{50}$-NRF_3:1**), 54.4% (**PVA$_{145000}$_PS$_{50}$-NRF_2:1**), and 61.15% (**PVA$_{145000}$_PS$_{50}$-NRF_1:1**), showing an increase as the polymer-to-NRF-loaded nanoparticle ratio decreased. Over the same time interval, the control samples **PVA$_{145000}$-NRF** exhibited a significantly faster release rate (**Figure 3.14.**). This result confirms the ability of the **PVA$_{145000}$_PS$_{50}$** system to incorporate drug-carrying nanoparticles and to release them via diffusion in a controlled manner, thereby improving bioavailability and reducing systemic toxicity.

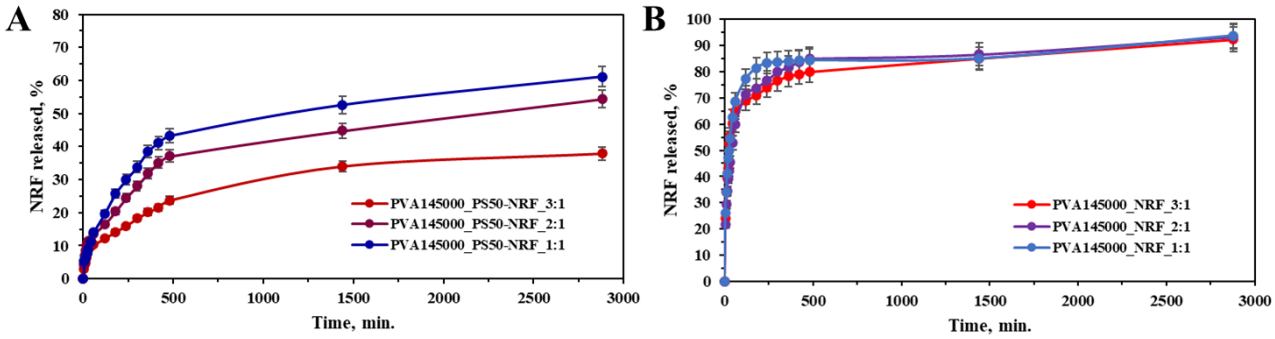

Figure 3.14. Release profiles of NRF from hydrogels based on (**A**) PVA$_{145000}$_PS$_{50}$-NRF and (**B**) PVA$_{145000}$.

CHAPTER IV. MULTICOMPONENT SYNTHETIC POLYMER-BASED HYDROGELS WITH ANTIBACTERIAL/ANTIOXIDANT INCLUSIONS

IV.1. Research background

The impact of the degree of bacterial contamination on the healing process of chronic wounds is not fully understood and is most likely underestimated. The presence of bacterial biofilm has been identified as a critical factor, and studies have shown a correlation between lesion depth and duration and the presence of *Staphylococcus* strains. Moreover, bacterial colonization of wounds (frequently caused by *S. aureus*, *P. aeruginosa*, *S. pyogenes*, and certain *Clostridium* strains) has been shown to further delay the healing process [170,171].

In this context, various strategies have been developed to enhance materials with antibacterial activity. One such approach involves loading hydrogels with antibacterial agents, such as natural extracts (phenolic compounds and essential plant oils), which can inhibit microbial growth on the material surface. Encapsulation of antibacterial bioactive compounds within a polymeric matrix offers multiple advantages, including protection against moisture, free radicals, and oxygen; prevention of undesirable chemical reactions between active species; modification of density, color, or photosensitivity; and increased system stability [9]. In addition, from an application perspective, this approach enables more efficient preservation and easier handling of active compounds while promoting their sustained release. Thus, it can ensure control over skin regeneration and reduce microbial contamination, which may otherwise hinder the healing process.

IV.2. Specific scientific objectives:

- Preparation of polymeric structures with a tunable hydrophilic/hydrophobic ratio capable of encapsulating hydrophobic bioactive compounds;
- Preparation of multicomponent hydrogels with antibacterial and antioxidant inclusions based on PVA, PEBSA, Thy, and α-Tcp;
- Characterization of the systems to obtain information regarding chemical composition, thermal stability, morphology, contact angle determination, and simulated biological fluid retention capacity; quantitative analysis of the released active compound; evaluation of antibacterial and antioxidant activity; *in vitro* cytotoxicity studies on the

BALB/3T3 clone A31 cell line; and *in vivo* studies regarding their applicability in skin wound healing.

Thy is a natural monoterpenoid phenol and one of the main active compounds found in essential oils extracted from *Thymus vulgaris* (thyme) and other plants such as *Ocimum gratissimum* L. (basil) or *Origanum* L. (oregano) [172]. Various pharmacological properties of these compounds have been reported, including antibacterial, antifungal, antioxidant, anti-inflammatory, analgesic, and wound-healing activities [173–176]. Thy has been shown to be effective against bacterial strains such as *S. aureus* and *E. coli*, as well as fungal strains such as *C. albicans*. Literature data indicate that phenols interact with polysaccharides, fatty acids, and phospholipids in the bacterial cell membrane structure, leading to the loss of cellular constituents and, ultimately, cell death [177–179].

α-Tcp, the most biologically active and effective form of vitamin E, is a potent liposoluble antioxidant responsible for protecting cells against oxidative stress and contributing to the mechanical stabilization of membranes through van der Waals-type physical interactions [105]. The supplementation of the PVA_PEBSA_Thy system with α-Tcp aimed to achieve a synergistic effect between the two bioactive compounds.

IV.3. Synthesis of poly(ethylene brassilate-co-squaric acid) copolymer

The PEBSA copolymer was synthesized via a ring-opening polymerization reaction between ethylene brassilate (EB) and squaric acid (SA), at EB:SA molar ratios of 25:75, 50:50, and 75:25, in the presence of 1-hexanol as initiator and 1,4-dioxane as solvent, using the method reported in the literature by Chiriac et al. [42] (**Figure 4.1.**). The reactions were carried out under a nitrogen atmosphere at a constant temperature of 100 °C, with magnetic stirring at 250 rpm for 24 h.

Purification of the final reaction mixture was performed through repeated wash–sedimentation cycles in diethyl ether and distilled water. The resulting product was frozen in liquid nitrogen and lyophilized for 24 h at −55 °C (Alpha 1-2LD Plus, Martin Christ, Germany).

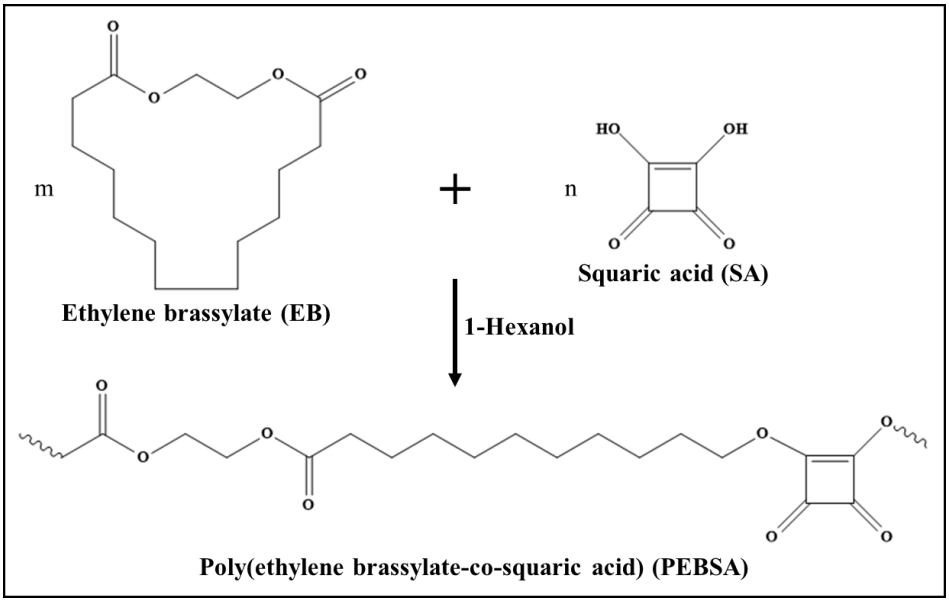

Figure 4.1. Schematic representation of the synthesis of the PEBSA copolymer [42].

IV.5. Preparation and characterization of multicomponent hydrogels based on synthetic polymers with antibacterial inclusions

The aim of the study was the preparation and characterization of multicomponent hydrogels based on PVA, PEBSA, and Thy, using the freeze–thaw technique, in order to confer antibacterial properties to the polymeric matrices obtained in subchapter IV.4.

IV.5.1. Preparation of PVA_PEBSA_Thy-based antibacterial hydrogels

The preparation of antibacterial hydrogels based on PVA with different molecular weights (72,000 and 145,000 g/mol), PEBSA with different molar ratios between the EB:SA comonomers (25:75, 50:50, and 75:25), and Thy involved two approaches: **(1) *in situ* entrapment of Thy during the gelation step** and **(2) Thy loaded into the preformed hydrogels** (**Figure 4.10.**) [187].

FTIR spectroscopy confirmed the structure of the multicomponent antibacterial hydrogels. The appearance of new signals in the 1620–1580 cm^{-1} region (C=C stretching) and 1290–1280 cm^{-1} region (C–O stretching) indicated the presence of the bioactive compound Thy. The release of Thy from the hydrogels exhibited a rapid initial phase within the first minutes, followed by a gradual release process extending up to 11–12 h in the case of systems containing $PEBSA_{25/75}$. A release exponent n lower than 0.5 for all samples suggested a quasi-Fickian diffusion mechanism, due to polymer relaxation, which is significantly higher than the diffusion

rate of the bioactive compound. The correlation coefficients (R^2) corresponding to the fitting curves used for the determination of n and K ranged between 0.9813 and 0.9997, approaching 1, indicating a good fit of all systems to the Korsmeyer–Peppas model.

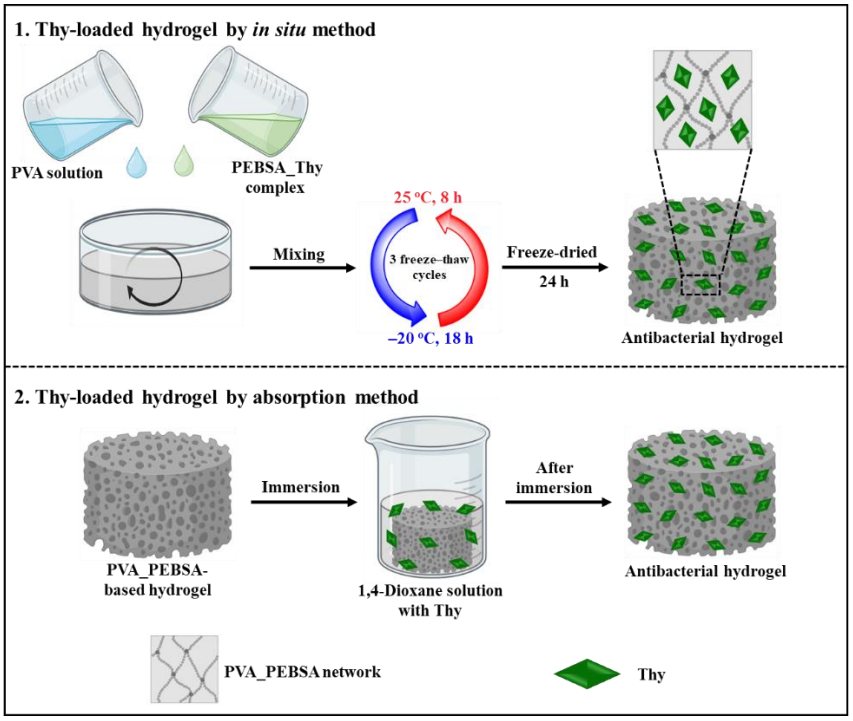

Figure 4.10. Schematic representation of the preparation steps of multicomponent hydrogels based on PVA_PEBSA_Thy [187].

IV.6. Preparation and characterization of multicomponent hydrogels based on synthetic polymers with antibacterial/antioxidant inclusions

The study aimed at the preparation and characterization of multicomponent hydrogels with antibacterial and antioxidant properties based on PVA, PEBSA, Thy, and α-Tcp, as well as the investigation of the synergistic potential between the two bioactive compounds, with a view to their application in the field of skin wound care and treatment.

IV.6.1. Preparation of PVA_PEBSA_Thy_α-Tcp antibacterial hydrogels

The PEBSA_Thy_α-Tcp complex was obtained by mixing a PEBSA solution (0.066 g/mL in 1,4-dioxane) with Thy and α-Tcp at PEBSA:Thy:α-Tcp gravimetric ratios of 1:1:1, 1:2:1, and 1:1:2, respectively, as shown in **Table 4.9.** In the second stage, the PEBSA_Thy_α-Tcp complex was mixed with a 4% PVA solution at a 2:1 volumetric ratio and subjected to freeze–thaw cycles (3 cycles consisting of 18 h freezing at −20 °C, followed by thawing for 8 h at room temperature). The obtained antibacterial hydrogels were lyophilized (24 h at −55 °C, Alpha 1-2LD Plus, Martin Christ, Germany) and stored in a desiccator at room temperature for further studies.

Table 4.9. Composition of PVA_PEBSA_Thy_α-Tcp-based systems.

Sample code*	PVA:PEBSA volumetric ratio	System composition for a total volume of 5 mL			
		PVA (g)	PEBSA (g)	Thy (g)	α-Tcp (g)
PVA_{72000}_$PEBSA_{25/75}$_ Thy_α-Tcp	2:1	0.132	0.066	0.066	0.066
PVA_{145000}_$PEBSA_{25/75}$_ Thy_α-Tcp				0.066	0.066
PVA_{72000}_$PEBSA_{50/50}$_ Thy_α-Tcp				0.066	0.066
PVA_{145000}_$PEBSA_{50/50}$_ Thy_α-Tcp				0.066	0.066
PVA_{72000}_$PEBSA_{75/25}$_ Thy_α-Tcp				0.066	0.066
PVA_{145000}_$PEBSA_{75/25}$_ Thy_α-Tcp				0.066	0.066
PVA_{72000}_$PEBSA_{50/50}$_ 2xThy_α-Tcp				0.132	0.066
PVA_{72000}_$PEBSA_{50/50}$_ Thy_2xα-Tcp				0.066	0.132

* 4% concentration for both polymer solutions

The shift of the absorption bands observed in the 1290–1280 cm^{-1} region (C–O stretching) and 852–809 cm^{-1} region (C=C bending) indicated the presence of the bioactive compound Thy (**Figure 4.18. B**). At the same time, the shift of the absorption bands confirmed the involvement of –OH, –C=O, and $–CH_3$ groups in the formation of intermolecular hydrogen bonds, as well as van der Waals interactions.

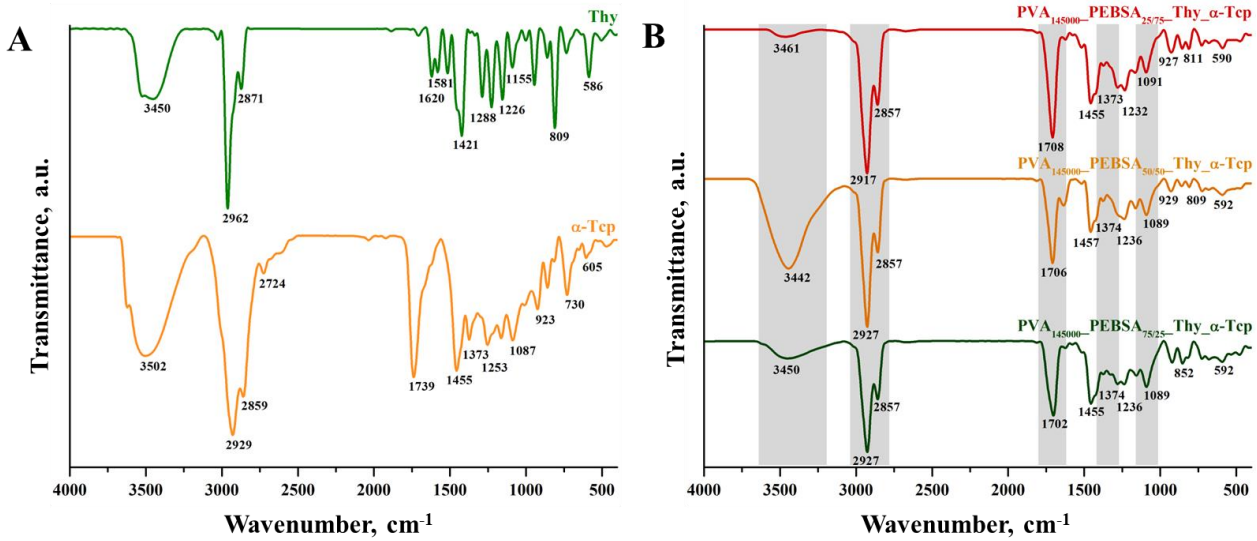

Figure 4.18. FTIR spectra of the samples: (**A**) Thy and α-Tcp, and

(**B**) PVA_{145000}_$PEBSA_{25/75}$_Thy_α-Tcp, PVA_{145000}_$PEBSA_{50/50}$_Thy_α-Tcp and PVA_{145000}_$PEBSA_{75/25}$_Thy_α-Tcp.

In order to ensure adequate absorption of wound exudate, the contact angle value of a dressing surface should be lower than 90° [196]. The water contact angle values ranged between 44° (**PVA_{72000}_$PEBSA_{50/50}$_Thy_α-Tcp**) and 64° (**PVA_{145000}_$PEBSA_{75/25}$_Thy_α-Tcp**), indicating a moderate hydrophilic character (**Figure 4.22.**). The experimental results suggested that hydrophobic segments are oriented toward the interior (hydrophobic core), while hydrophilic segments surround the core, stabilizing the outer structure (hydrophilic shell).

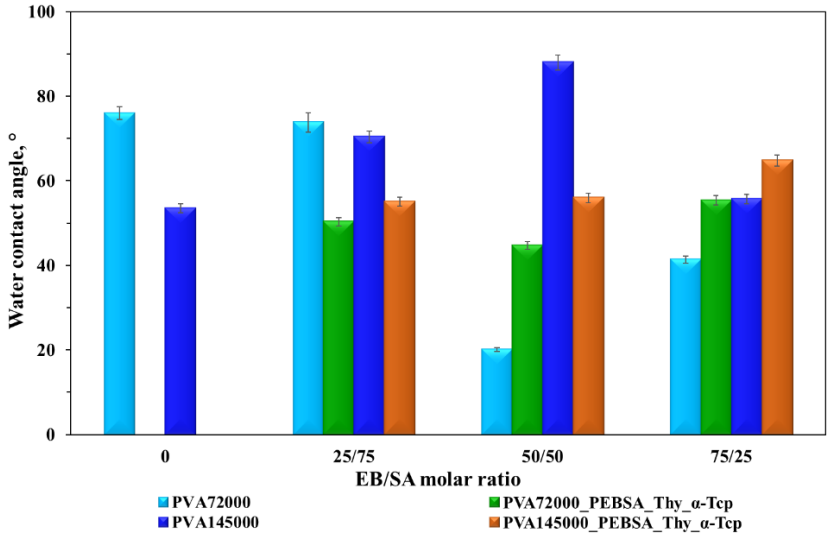

Figure 4.22. Water contact angle values on the surface of PVA- and PEBSA-based films with and without Thy_α-Tcp. Results are expressed as mean ± standard deviation.

The cumulative release profiles of Thy and α-Tcp confirmed the ability of the PVA_PEBSA system to incorporate and release the bioactive compounds in a controlled manner at pH 5.4 and 7.4. Antibacterial activity against *S. aureus*, *E. coli*, and *C. albicans* was evaluated using the Kirby–Bauer method. The results of the antibacterial activity testing of the multicomponent PVA_PEBSA_Thy_α-Tcp hydrogels are presented in **Table 4.12.**

Table 4.12. Diameter of inhibition zones (mm) of the tested systems.

Sample code	Inhibition zone diameter (mm)*		
	S. aureus	***E. coli***	***C. albicans***
PVA_{72000}_$PEBSA_{25/75}$_Thy_α-Tcp	22.30 ± 0.14	21.90 ± 0.99	38.55 ± 1.48
PVA_{72000}_$PEBSA_{50/50}$_Thy_α-Tcp	21.10 ± 0.00	19.15 ± 1.06	32.25 ± 3.18
PVA_{72000}_$PEBSA_{75/25}$_Thy_α-Tcp	25.90 ± 0.70	25.45 ± 3.46	34.65 ± 0.91
PVA_{72000}_$PEBSA_{50/50}$_2xThy_α-Tcp	27.05 ± 0.63	28.40 ± 0.14	37.80 ± 0.28
PVA_{72000}_$PEBSA_{50/50}$_Thy_2xα-Tcp	21.80 ± 3.25	19.20 ± 0.00	28.25 ± 0.77

* Results are presented as mean ± standard deviation.

The systems exhibited antibacterial activity against the growth of the reference strains. The fungal strain *C. albicans* showed high sensitivity to all tested systems, with inhibition zone diameters ranging from 28.25 ± 0.77 mm (**PVA_{72000}_$PEBSA_{50/50}$_Thy_2xα-Tcp**) to 38.55 ± 1.48 mm (**PVA_{72000}_$PEBSA_{25/75}$_Thy_α-Tcp**). According to the results obtained from the DPPH radical scavenging assay, all samples exhibited antioxidant activity (**Figure 4.28.**). The carbonyl functional groups of SA are arranged in a configuration favorable for electron transfer, and consequently, a higher SA monomer content (75%) leads to an increased free radical (DPPH) scavenging activity.

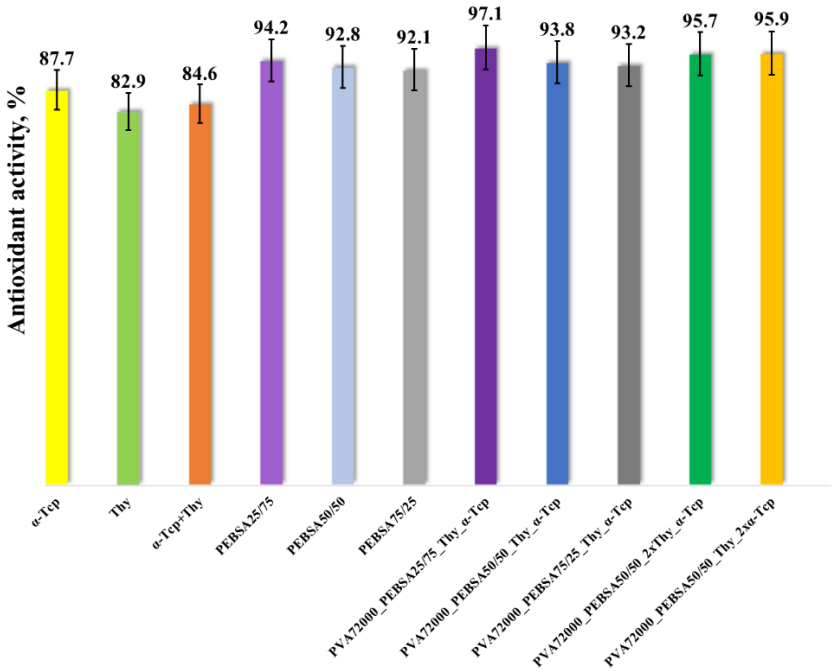

Figure 4.28. Antioxidant activity of PVA_{72000}_PEBSA_Thy_α-Tcp systems compared with control samples. Results are expressed as mean ± standard deviation.

The 3-(4,5-dimethylthiazol-2-yl)-2,5-diphenyltetrazolium bromide (MTT) assay indicated the absence of cytotoxicity of the antibacterial materials toward fibroblasts from the BALB/3T3 clone A31 cell line, with cell viability values exceeding 90% for all three exposure times (24, 48, and 72 h). Phase-contrast and fluorescence microscopy of cell morphology confirmed the cytocompatibility of the samples, showing no negative effects on cell attachment or proliferation.

The property of polymeric systems not to induce any inflammatory response in living tissue upon contact [215] was evaluated by subcutaneous implantation of antibacterial hydrogels in female Wistar rats. The experimental procedures were carried out in accordance with the 3R principles, aiming to reduce the number of animal tests; thus, due to the limited number of

available animals and according to subchapter *II.2 Methods of analysis*, a selection of samples was performed. Superior antibacterial activity against *C. albicans* (inhibition zone diameters up to 38 mm), high antioxidant properties (97.1%), and moderate hydrophilicity (~55° contact angle) led to the selection of **PVA_{72000}_$PEBSA_{25/75}$_Thy_α-Tcp** antibacterial hydrogels as the experimental group. The **PVA_{72000}_$PEBSA_{25/75}$** matrix was considered as the control group.

The study was conducted over a period of 21 days, during which animal welfare, food and water intake, as well as the condition of the fur and mucous membranes, were carefully monitored in order to detect possible adverse reactions [211]. The tested materials did not cause animal mortality, and no cases of visible inflammation in the dorsal region were observed, nor any behavior associated with pain, according to the Grimace scale and body weight monitoring of the animals (**Figure 4.31. N**). Moreover, the subcutaneously implanted materials exhibited swelling behavior over time while maintaining their rectangular shape (**Figure 4.31. M**).

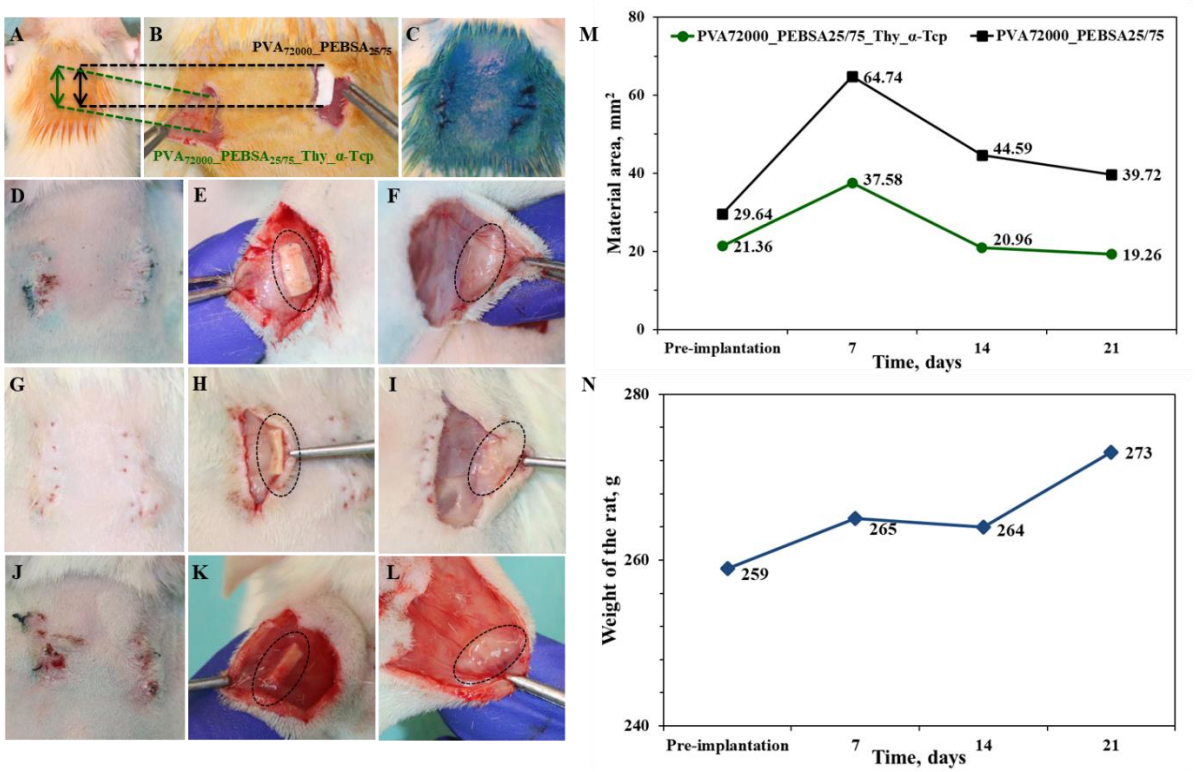

Figure 4.31. Experimental procedure for subcutaneous implantation of multicomponent hydrogels: (**A**) preparation of the dorsal skin region; (**B**) subcutaneous placement of the test samples; (**C**) suturing and aseptic closure of the incisions; implanted materials observed subcutaneously at (**D**–**F**) 7 days, (**G**–**I**) 14 days, and (**J**–**L**) 21 days; (**M**) time-dependent area variation of PVA_{72000}_$PEBSA_{25/75}$_Thy_α-Tcp and PVA_{72000}_$PEBSA_{25/75}$ samples; and (**N**) body weight monitoring of the animals over 21 days.

The applicability of the **PVA$_{72000}$_PEBSA$_{25/75}$_Thy_α-Tcp** antibacterial hydrogels in skin wound healing was evaluated in rats of the same strain. The wound healing process was assessed by measuring the lesion area at predefined monitoring time points (**Figure 4.32.**) [211]. At 20 days after wound induction, almost complete healing was observed (99.36% and 94.91%) in the groups treated with the multicomponent hydrogels.

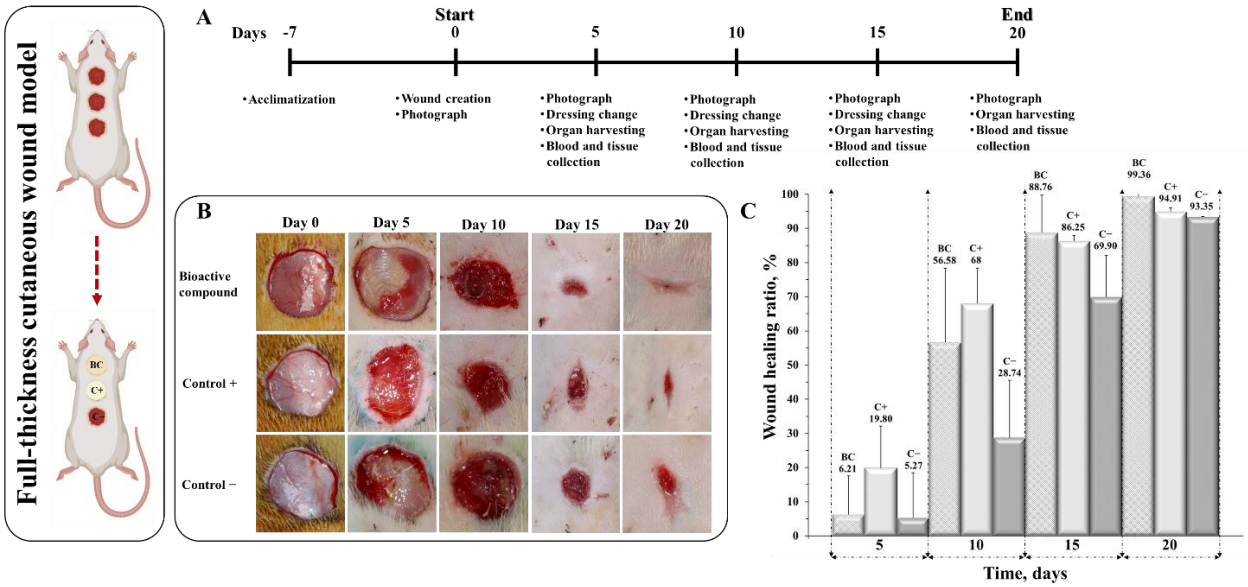

Figure 4.32. (**A**) Experimental procedure regarding the applicability of antibacterial hydrogels in cutaneous wound healing; (**B**) images of the wound healing process upon application of the antibacterial material (BC) and the positive control (C+) compared with the negative control (C−); (**C**) wound healing capacity at days 5, 10, 15, and 20 after the start of the study. Results are expressed as mean ± standard deviation.

Interleukin-8 (IL-8) plays a role in attracting neutrophils to the site of inflammation and is often evaluated for the early detection of inflammatory lesions in regions in contact with test samples [216]. Subcutaneous implantation of the materials (**PVA$_{72000}$_PEBSA$_{25/75}$_Thy_α-Tcp** and **PVA$_{72000}$_PEBSA$_{25/75}$**) did not induce significant variations in serum IL-8 levels (32.34 ± 0.33, 27.96 ± 4.23, and 31.12 ± 1.58 pg/mL) compared to the control group (28.45 ± 2.55 pg/mL) at 7, 14, and 21 days after the onset of the experiment, confirming their potential applicability in wound healing. The same trend was observed in the experimental group used for wound healing assessment, where IL-8 concentrations were 26.51 ± 4.32, 25.79 ± 2.31, 24.59 ± 2.75, and 27.04 ± 4.77 pg/mL at 5, 10, 15, and 20 days after wound induction, respectively.

CHAPTER V. HYBRID ANTIBACTERIAL HYDROGELS

V.1. Research background

Synthetic polymers are relatively easy to synthesize, even on a large scale, through specific production processes, allowing modification reactions that ensure further diversity in their applications. Their chemical structure, molecular weight, and physicochemical properties (mechanical strength, biodegradability), as well as their reproducibility, are of major importance for biomedical applications. The use of synthetic polymers as biomaterials is limited by their lack of intrinsic bioactivity. In addition to the remarkable advantages of natural polymers (bioactivity, biodegradability, biocompatibility), they also present certain drawbacks (poor mechanical properties, lack of reproducibility). These limitations can be overcome by using synthetic polymers. By combining the properties of synthetic and natural polymers in *hybrid structures*, systems with superior properties compared to each individual polymer class can be obtained [18,19].

Among the many available natural polymers, **dextran** and **xanthan gum** are the subject of experimental studies on the preparation of multicomponent hybrid hydrogels based on natural/synthetic polymers using the freeze–thaw technique, due to their favorable physicochemical and biofunctional characteristics for applications in tissue engineering and regenerative medicine.

Dextran is a highly water-soluble polysaccharide produced through the enzymatic synthesis of bacteria from the genera *Leuconostoc* and *Streptococcus*. Chemically, it consists of repeating glucose units linked by α-(1→6) glycosidic bonds. Its polymeric structure, biocompatibility, biodegradability, and hydrophilic properties make it an excellent choice for applications targeting the development of hydrogel-based wound dressings [217,218].

Xanthan gum is an anionic heteropolysaccharide obtained through the fermentation of carbohydrates using the bacterium *Xanthomonas campestris*. Chemically, it is composed of repeating units of D-glucose, D-mannose, and D-glucuronic acid in a molar ratio of 3:3:2 [219]. Due to its hydrophilic character, good stability over a wide range of pH values and temperatures, and the presence of reactive functional groups (–OH, –COOH, $–CH_2OH$, $–CH_3$), xanthan gum is used in the preparation of hydrogels for applications in skin tissue engineering [220].

Literature data indicate that dextran exhibits significant bioactivity by stimulating angiogenic responses and facilitating tissue regeneration during the wound healing process

[49,50]. The negatively charged carboxyl functional groups present in xanthan gum can significantly reduce inflammatory responses and are effective in promoting fibroblast adhesion [221,222]. Some formulations may also exhibit antibacterial properties, which can help prevent or reduce the risk of infections [223].

V.2. Specific scientific objectives:

- Preparation of multicomponent hybrid hydrogels with antibacterial inclusions based on PVA, PEBSA, dextran or xanthan gum, and Amx;
- Characterization of the systems to obtain information regarding chemical composition, thermal stability, morphology, determination of simulated biological fluid retention capacity, *in vitro* enzymatic degradation studies, quantitative analysis of the released active compound, evaluation of antibacterial activity, and *in vitro* studies on normal human dermal fibroblast cultures.

Amx is an antibiotic belonging to the β-lactam class, a penicillin derivative with higher bioavailability and an extended antibacterial spectrum. It exhibits efficacy against a wide range of Gram-positive and Gram-negative bacterial strains [224], including *S. aureus*, *S. pneumoniae*, *E. coli*, and *Haemophilus influenzae* (*H. influenzae*). The antibacterial mechanism of Amx, as reported in the literature, involves the inhibition of bacterial cell wall synthesis [60].

V.4. Preparation and characterization of multicomponent hybrid hydrogels with antibacterial inclusions

The aim of the study was the preparation and characterization of multicomponent hybrid hydrogels based on PVA, PEBSA, dextran or xanthan gum, and Amx, using the freeze–thaw technique, in order to confer antibacterial properties to the polymeric matrices. The introduction of the two polysaccharides into the PVA_{72000}_PEBSA-based polymer systems aimed to develop hybrid materials with advanced properties for regenerative medicine applications, such as increased bioadhesiveness, controlled morphology, high swelling capacity, and effective conformability to wound geometry. At the same time, the study considered achieving controlled biodegradability in a biological environment, as well as ensuring optimal biocompatibility under *in vivo* conditions.

V.4.1. Preparation of PVA_PEBSA_Dextran_Amx hybrid antibacterial hydrogels

The preparation of PVA_PEBSA_Dextran_Amx hybrid antibacterial hydrogels was carried out in a stepwise manner, with the first stage focusing on the formation of the PEBSA_Dextran_Amx network (**Figure 5.11.**). This was obtained by separately preparing a PEBSA solution (0.016 g/mL in 1,4-dioxane) containing Amx (0.03 g) and a 10% dextran solution, followed by mixing the two solutions at a PEBSA:polysaccharide volumetric ratio of 1:3. The hybrid systems were then obtained by adding a 4% PVA_{72000} solution and subjecting the mixtures to three freeze–thaw cycles in order to form the second network. Three hydrogel variants with different compositions were obtained, as listed in **Table 5.5.** The samples were lyophilized (48 h at −55 °C, Alpha 1-2LD Plus, Martin Christ, Germany) and stored in a desiccator at room temperature for further studies.

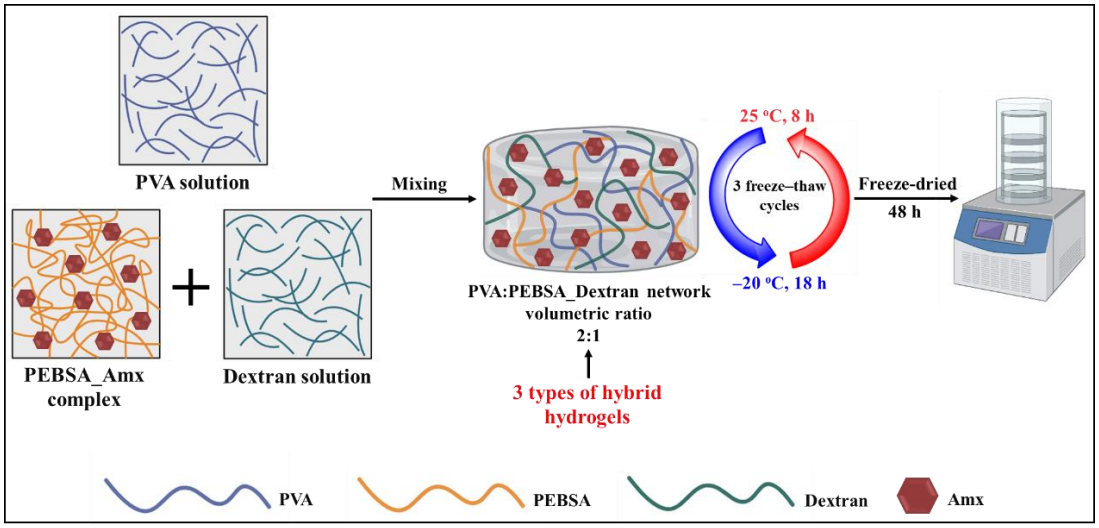

Figure 5.11. Schematic representation of the preparation steps of hybrid hydrogels based on PVA_PEBSA_Dextran_Amx.

Table 5.5. Composition of PVA_PEBSA_Dextran_Amx hybrid systems.

Sample code*	PVA:PEBSA_Dextran network volumetric ratio	System composition for a total volume of 5 mL			
		PVA (g)	PEBSA (g)	Dextran (g)	Amx (g)
PVA_{72000}_$PEBSA_{25/75}$_ Dextran_Amx	2:1	0.132	0.016	0.1249	0.03
PVA_{72000}_$PEBSA_{50/50}$_ Dextran_Amx					
PVA_{72000}_$PEBSA_{75/25}$_ Dextran_Amx					

* 4% concentration for the PVA_{72000} and PEBSA solutions, respectively, and 10% concentration for the dextran solution

FTIR spectroscopy data confirmed the presence of antibacterial inclusions within the structure of the hybrid hydrogels, as well as the interactions between the components of the polymer networks. The quantitative analysis of released Amx was performed based on the ^{1}H NMR spectra of the extracted solutions collected at predefined time intervals (30 min, 1, 2, 4, 22, 46, and 94 h). Drug quantification was achieved by proportional comparison between the reference signal (TSP at $\delta = 0$ ppm) and a selected signal assigned to Amx (e.g., the aryl signal at $\delta = 7.35$ ppm), based on the assumption that, in a proton NMR spectrum, signal integrals are directly proportional to the number of protons present in the sample volume [140] (**Figure 5.14. B**). It can be observed that all samples exhibit a biphasic release profile, characterized by an initial rapid release stage within the first 120–240 minutes, followed by a gradual release process that extended up to 94 h.

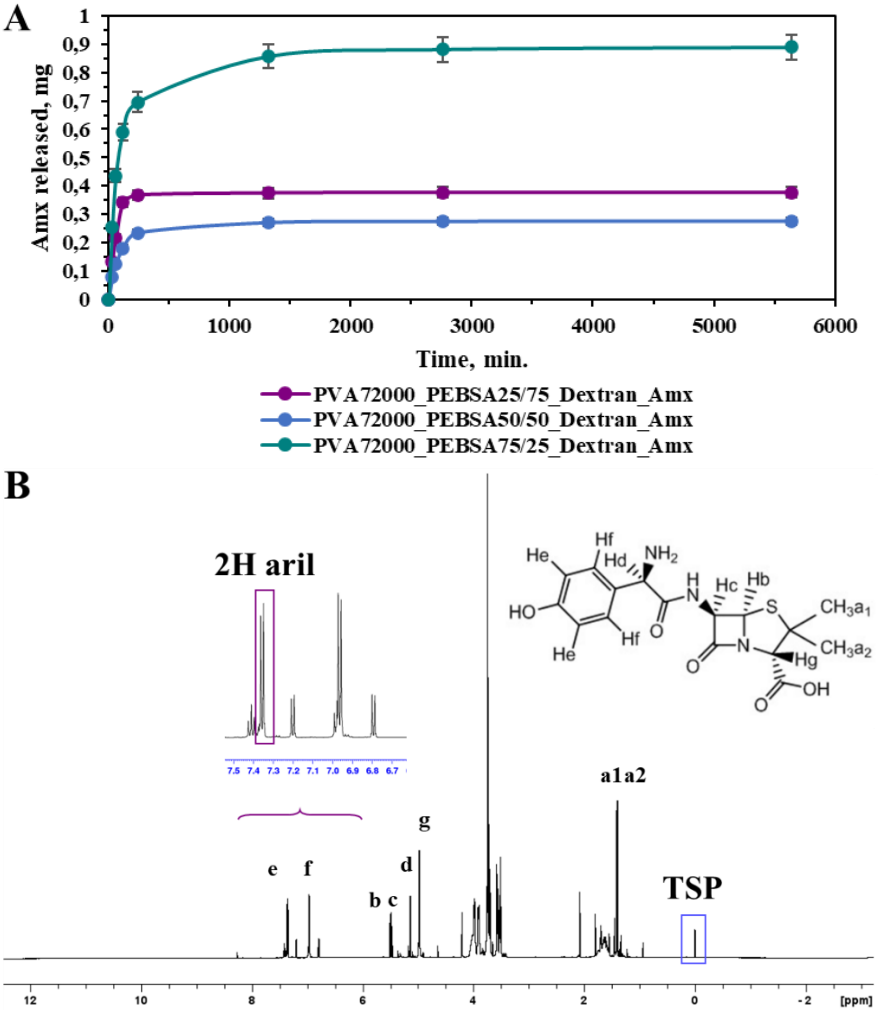

Figure 5.14. (**A**) Release profiles of Amx (mg) from hybrid hydrogels based on PVA_{72000}_PEBSA_Dextran_Amx in phosphate-buffered saline solution at pH = 7.4 and 0.01

M concentration, and (**B**) ^{1}H NMR spectrum @ 600 MHz of the PVA_{72000}_$PEBSA_{25/75}$_Dextran_Amx system.

The results of the antibacterial activity tests of the PVA72000_PEBSA_Dextran_Amx hybrid hydrogels, as evidenced by the inhibition zones against *S. aureus* (Gram-positive bacterial strain), *E. coli* (Gram-negative bacterial strain), *K. pneumoniae* (Gram-negative bacterial strain), and *E. faecalis* (Gram-positive bacterial strain), are presented in **Table 5.7.** *E. coli* exhibited high sensitivity to all Amx-loaded hybrid hydrogels, with inhibition zone diameters ranging from 32.53 ± 2.71 mm (**PVA_{72000}_$PEBSA_{25/75}$_Dextran_Amx**) to 34.86 ± 2.65 mm (**PVA_{72000}_$PEBSA_{75/25}$_Dextran_Amx**).

Table 5.7. Diameter of inhibition zones (mm) of the tested systems.

Sample code	Inhibition zone diameter (mm)*			
	S. aureus	***E. coli***	***K. pneumoniae***	***E. faecalis***
PVA_{72000}_$PEBSA_{25/75}$_Dextran	–	–	–	–
PVA_{72000}_$PEBSA_{50/50}$_Dextran	–	–	–	–
PVA_{72000}_$PEBSA_{75/25}$_Dextran	–	–	–	–
PVA_{72000}_$PEBSA_{25/75}$_ Dextran_Amx	24.03 ± 1.36	32.53 ± 2.71	17.90 ± 2.60	–
PVA_{72000}_$PEBSA_{50/50}$_ Dextran_Amx	23.23 ± 1.01	33.30 ± 1.38	20.13 ± 1.09	–
PVA_{72000}_$PEBSA_{75/25}$_ Dextran_Amx	23.66 ± 0.81	34.86 ± 2.65	19.80 ± 1.83	–

* Results are presented as mean ± standard deviation; (–) indicates no antibacterial activity.

Figure 5.17. presents cell viability expressed relative to the absorbance recorded in the control culture. The presence of polysaccharide contributed to an increase in cell viability compared to the **PVA_{72000}_$PEBSA_{75/25}$** matrices, whose cell viability was previously evaluated at approximately 92%. Moreover, the viability of normal human dermal fibroblasts following contact with the **PVA_{72000}_$PEBSA_{75/25}$_Dextran_Amx** systems exceeded 100%, demonstrating that these antibacterial materials are capable of supporting cell proliferation. Subsequently, the cells were analyzed by Calcein-AM staining to assess the influence of the materials on cell morphology. Microscopy images obtained at 10× magnification highlight the presence of viable cells and confirm the MTT assay results (**Figure 5.18.**). The cells maintained their morphological integrity and formed a uniform monolayer. Furthermore, the cell culture exhibited active proliferation, as evidenced by fibroblasts with a spindle-shaped morphology, characteristic of normal human dermal fibroblasts [241]. These results demonstrate that the

antibacterial hybrid hydrogels **PVA$_{72000}$_PEBSA$_{75/25}$_Dextran_Amx** are cytocompatible materials and promote cell proliferation.

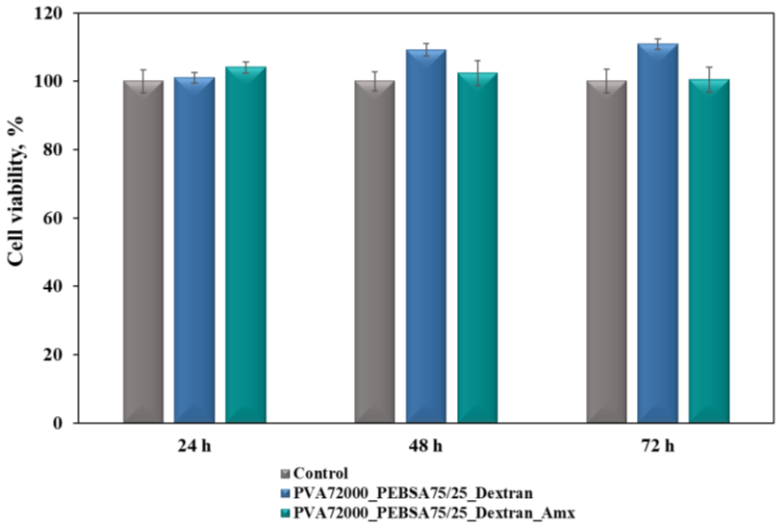

Figure 5.17. Viability of normal human dermal fibroblasts following contact with PVA$_{72000}$_PEBSA$_{75/25}$_Dextran and PVA$_{72000}$_PEBSA$_{75/25}$_Dextran_Amx samples at 24, 48, and 72 h. Results are expressed as mean ± standard deviation.

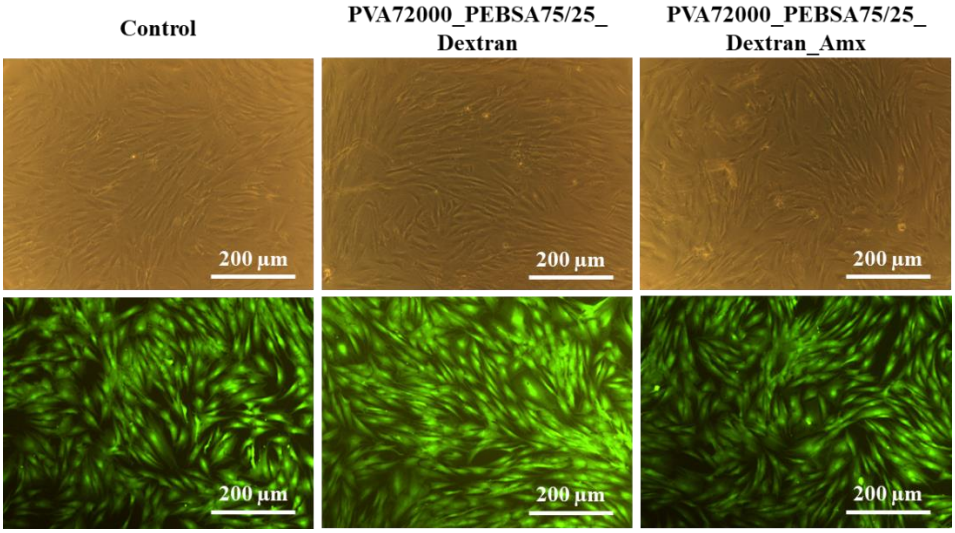

Figure 5.18. Morphology of fibroblasts under phase-contrast and fluorescence microscopy after 72 h of contact with PVA$_{72000}$_PEBSA$_{75/25}$_Dextran and PVA$_{72000}$_PEBSA$_{75/25}$_Dextran_Amx samples, respectively (10×).

V.4.4. Preparation of antibacterial hybrid hydrogels based on PVA_PEBSA_Xanthan gum_Amx

The same preparation protocol described in subsection *V.4.1. Preparation of antibacterial hybrid hydrogels based on PVA_PEBSA_Dextran_Amx*, was used.

Table 5.8. Composition of PVA_PEBSA_Xanthan gum_Amx hybrid systems.

Sample code*	PVA:PEBSA_ Xanthan gum network volumetric ratio	System composition for a total volume of 5 mL			
		PVA (g)	PEBSA (g)	Xanthan gum (g)	Amx (g)
PVA_{72000}_$PEBSA_{25/75}$_ Xanthan gum_Amx	2:1	0.132	0.016	0.0124	0.03
PVA_{72000}_$PEBSA_{50/50}$_ Xanthan gum_Amx					
PVA_{72000}_$PEBSA_{75/25}$_ Xanthan gum_Amx					

* 4% concentration for the PVA_{72000} and PEBSA solutions, respectively, and 1% concentration for the Xanthan gum solution

To describe the release mechanism of Amx from the **PVA_{72000}_PEBSA_Xanthan gum_Amx** hybrid hydrogels, the experimental data were fitted to four mathematical models: the zero-order model (8), the first-order model (9), the Higuchi model (10), and the Korsmeyer–Peppas model (6). Due to a better fit ($R^2 > 0.9$), only the results corresponding to the Higuchi and Korsmeyer–Peppas models are presented (**Figure 5.25.** and **Table 5.9.**).

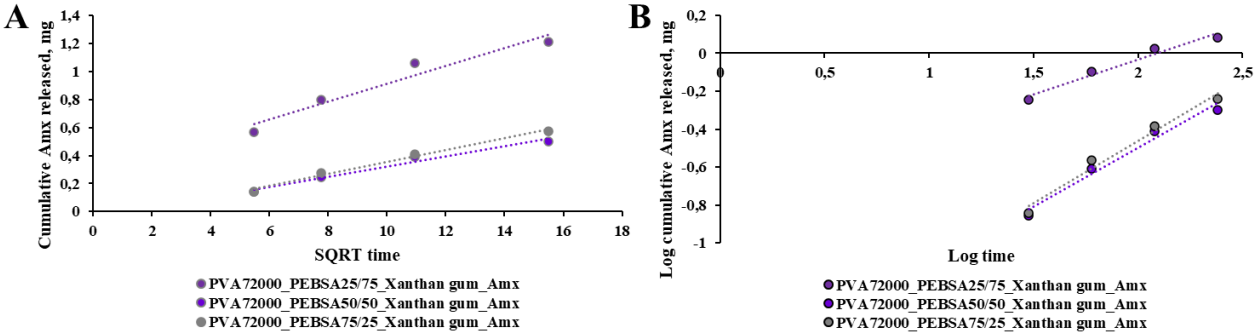

Figure 5.25. Amx release kinetics according to the (**A**) Higuchi and (**B**) Korsmeyer–Peppas models.

Table 5.9. Kinetic parameters for Amx release.

Sample code	Higuchi		Korsmeyer–Peppas		
	k	R^2	n	k_H	R^2
PVA_{72000}_$PEBSA_{25/75}$_ Xanthan gum_Amx	0.0635	0.9408	0.3689	0.7705	0.9668
PVA_{72000}_$PEBSA_{50/50}$_ Xanthan gum_Amx	0.0362	0.9767	0.6195	1.7373	0.9737
PVA_{72000}_$PEBSA_{75/25}$_ Xanthan gum_Amx	0.0423	0.9898	0.3689	0.7705	0.9664

The **PVA$_{72000}$_PEBSA$_{25/75}$_Xanthan gum_Amx** system correlated with the Korsmeyer–Peppas kinetic model. The value of the release exponent *n* (< 0.5 for this sample) suggested a quasi-Fickian mechanism influenced by polymer relaxation processes. In the case of the **PVA$_{72000}$_PEBSA$_{50/50}$_Xanthan gum_Amx** and **PVA$_{72000}$_PEBSA$_{75/25}$_Xanthan gum_Amx** systems, the Amx release kinetics are described by the Higuchi model (R^2 = 0.9767–0.9898). Phase-contrast and fluorescence microscopy images (**Figure 5.29.**) highlighted the dynamics of the cell migration process. In the presence of the **PVA$_{72000}$_PEBSA$_{75/25}$_Xanthan gum_Amx** samples, a visible closure of the cell defect was observed at 24 h after the onset of the experiment, a phenomenon already evident at 6 h and maintained until complete closure of the scratch area. The obtained results confirm that the antibacterial hybrid hydrogels are not only cytocompatible, but also promote key processes essential for tissue regeneration, such as fibroblast migration and proliferation.

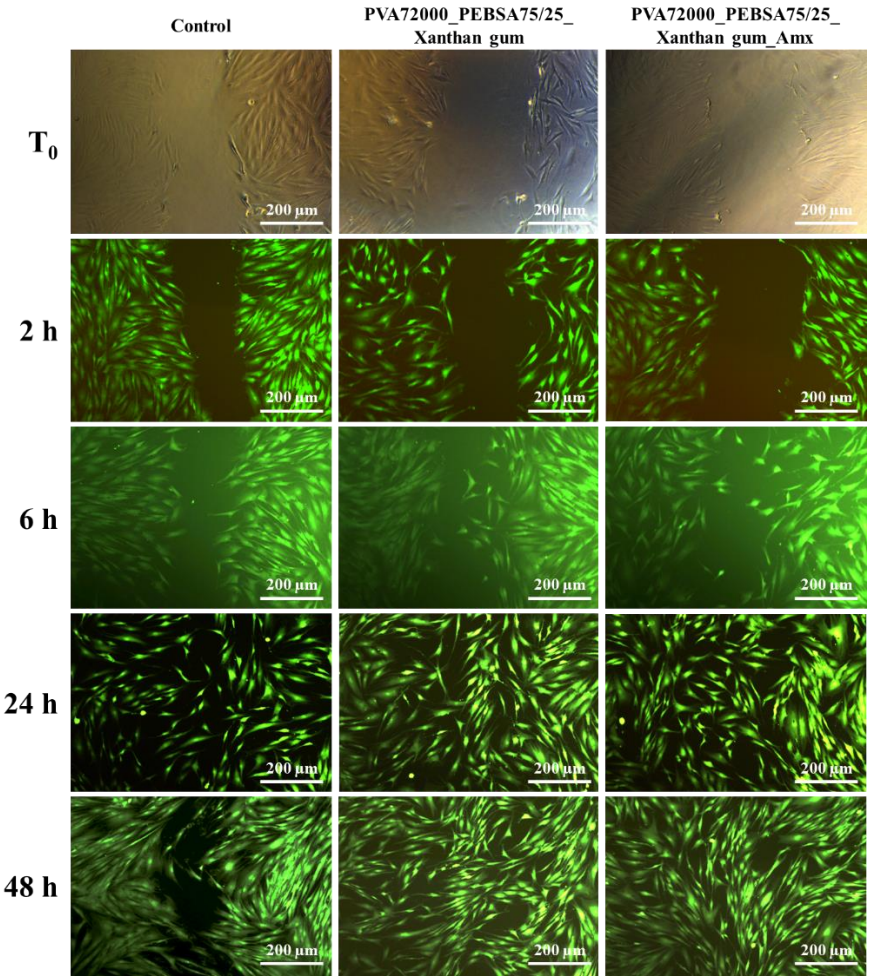

Figure 5.29. *In vitro* evaluation of the effect of PVA$_{72000}$_PEBSA$_{75/25}$_Xanthan gum and PVA$_{72000}$_PEBSA$_{75/25}$_Xanthan gum_Amx samples on cell migration capacity (10×).

CHAPTER VI. CONCLUSIONS

The doctoral thesis entitled "**Complex polymer matrices with antibacterial inclusions**" aimed to bring ***original contributions to the development of new polymeric structures with a tunable hydrophilic/hydrophobic ratio, based on synthetic and/or natural polymers, capable of improving the solubility, stability, and bioavailability of hydrophobic antibacterial agents for cutaneous applications***.

The objectives of the doctoral thesis were structured around three main research directions:

(i) the preparation and characterization of drug-loaded hydrogel systems based on **PVA**, **PEB**, and **NRF**;

(ii) the preparation and characterization of multicomponent hydrogels with antibacterial and antioxidant inclusions based on **PVA**, **PEBSA**, **Thy**, and **α-Tcp**;

(iii) the preparation and characterization of multicomponent hybrid hydrogels with antibacterial inclusions based on **PVA**, **PEBSA**, **dextran** or **xanthan gum**, and **Amx**.

The conducted studies enabled the systematization of the following conclusions:

Synthesis and physico-chemical characterization of PEB homopolymer

- Six homopolymer syntheses were performed using both bulk and solution (1,4-dioxane) polymerization methods, in the presence of 1-hexanol as initiator and two organic catalysts, PTSA and TBD. In order to characterize the EB polymerization reaction, two key parameters were investigated: monomer conversion into homopolymer and molecular weight distribution.
- The 1-hexanol/TBD system proved to be the most efficient promoter of the ring-opening polymerization of EB, at an EB:TBD molar ratio of 50:1.
- Spectroscopic analyses (FTIR and ^{1}H NMR) confirmed the chemical structure of the synthesized homopolymers.
- XRD investigations indicated a crystallinity degree of approximately 57.2%, while the average crystallite size was estimated at 25.3 nm.
- Thermogravimetric data revealed a single-step degradation process, with a maximum thermal degradation temperature (T_{peak}) of approximately 454 °C and a residual mass of 1.16%.

The study demonstrated the feasibility of synthesizing PEB homopolymer through sustainable methods, achieving conversions above 70% under mild reaction conditions, the process being adapted to the requirements of biomedical applications.

Homopolymer–drug nanoparticle systems based on PEB

- Four types of nanoparticulate systems based on PEB were obtained via the precipitation method, with NRF being incorporated *in situ* into the homopolymeric matrix.
- DLS investigations showed that the hydrodynamic diameter of the nanoparticles is influenced by the molecular weight distribution of the corresponding PEB homopolymers, with sizes ranging between 190.6–290.7 nm.
- The encapsulation efficiency was determined to be 35.98% for **PS_{100}-NRF**, 39.87% for **PS_{150}-NRF**, and 44.84% for **PS_{50}-NRF**. This result is explained by the higher hydrophobic affinity of the **PEB_{50}_TBD** homopolymer for the encapsulation of NRF molecules.
- STEM microscopy revealed that nanoparticles based on PEB_{50}_TBD (**PS_{50}**) exhibit a morphology favorable for use as drug delivery systems. The **PS_{50}-NRF** nanoparticles displayed a core–shell structure and a significantly enhanced contrast due to drug loading.

The correlation of the obtained results enabled the selection of the PEB_{50}_TBD variant, synthesized via solution polymerization, for the development of nanocarriers capable of incorporating hydrophobic bioactive compounds. This choice was also supported by the conversion studies, which indicated a monomer-to-homopolymer conversion degree of approximately 83% for this sample.

PVA-based hydrogels loaded with drug carrier nanoparticles

- Three PVA-based hydrogels loaded with drug carrier nanoparticles were obtained using the freeze–thaw technique.
- Structural characterization by FTIR spectroscopy confirmed the structure of the **PVA_{145000}_PS_{50}-NRF** hydrogels. The shifts in absorption bands confirmed the involvement of –OH, –NH–, and –C=O groups in the formation of intermolecular physical interactions.

- SEM images highlighted the formation of well-defined porous networks with interconnected pores, which differed in terms of density, distribution, and size.
- The swelling behavior of the polymer matrices was dependent on the PVA:PS_{50}-NRF volumetric ratio and morphological characteristics, reaching a maximum of 1160% for **PVA_{145000}_PS_{50}_2:1**.
- The maximum amount of antibiotic released over 48 h was 37.83% (**PVA_{145000}_PS_{50}-NRF_3:1**), 54.4% (**PVA_{145000}_PS_{50}-NRF_2:1**), and 61.15% (**PVA_{145000}_PS_{50}-NRF_1:1**).

The study confirmed the potential of the PVA_{145000}_PS_{50} system to incorporate drug carrier nanoparticles and to ensure controlled release via a diffusion mechanism under *in vitro* conditions.

Antibacterial hydrogels based on PVA_PEBSA_Thy

- Eight hydrogels with a tunable hydrophilic/hydrophobic ratio were obtained based on PVA with different molecular weights (72,000 and 145,000 g/mol), PEBSA with different molar ratios between the EB:SA comonomers (25:75, 50:50, and 75:25), and Thy, using two approaches: (1) *in situ* incorporation of Thy and (2) incorporation of Thy by absorption into preformed hydrogels.
- FTIR spectroscopy data revealed that the most effective interaction with Thy is observed in systems containing $PEBSA_{25/75}$, as a result of intermolecular physical interactions formed between the bioactive compound and the carbonyl functional groups in SA.
- Thermogravimetric analysis showed that *in situ* incorporation of Thy leads to an increase in thermal stability.
- Morphological characterization by SEM microscopy evidenced a relatively uniform distribution of the bioactive compound both within the polymer matrix and in the pore spaces in the case of hydrogels loaded via absorption. Swelling in 1,4-dioxane containing Thy induced network relaxation and pore expansion, thereby facilitating the complete uptake of Thy molecules.
- The release of Thy from the hydrogels exhibited a rapid initial phase within the first minutes, followed by a gradual release process extending up to 11–12 h in the case of PVA_$PEBSA_{25/75}$-based systems. The data suggested a quasi-Fickian diffusion mechanism and good fitting to the Korsmeyer–Peppas model.

- All PVA_PEBSA_Thy systems, regardless of the incorporation method of the bioactive compound, exhibited antibacterial activity against *S. aureus* (Gram-positive bacterial strain), *E. coli* (Gram-negative bacterial strain), and *C. albicans* (fungal strain).

The obtained results suggest that PVA_PEBSA$_{25/75}$_Thy hydrogels present favorable characteristics for potential use as wound dressing materials.

Antibacterial hydrogels based on PVA_PEBSA_Thy_α-Tcp

- Eight hydrogels with a tunable hydrophilic/hydrophobic ratio, based on PVA, PEBSA, Thy, and α-Tcp, were prepared using the freeze–thaw technique. The incorporation of α-Tcp into the PVA_PEBSA_Thy system was intended to achieve a synergistic effect between the two bioactive compounds.
- FTIR spectroscopy confirmed the structure of the multicomponent antibacterial PVA_PEBSA_Thy_α-Tcp hydrogels.
- The morphology of the PVA_PEBSA_Thy_α-Tcp systems revealed a relatively uniform distribution of the bioactive compounds (Thy and α-Tcp) over the surface of the polymer network. This behavior was attributed to the compatibility between the amphiphilic PEBSA copolymer and the hydrophobic bioactive compounds.
- AFM investigations demonstrated that the PVA_PEBSA systems exhibit roughness parameter values suitable for the use of polymeric hydrogels in controlled drug delivery applications.
- Contact angle measurements indicated that the hydrophilic/hydrophobic character can be tailored by adjusting the ratios between the blending components, particularly the molar ratio of the EB:SA comonomers.
- The cumulative release profiles of Thy and α-Tcp confirmed the ability of the PVA_PEBSA system to incorporate and provide controlled and sustained release of the bioactive compounds under simulated physiological conditions.
- All PVA_PEBSA_Thy_α-Tcp systems exhibited a bacteriostatic effect against the growth of *S. aureus*, *E. coli*, and *C. albicans*.
- The cumulative antioxidant activity of Thy and α-Tcp, in association with PEBSA, produced a notable synergistic effect, ranging from 93.2% (**PVA$_{72000}$_PEBSA$_{75/25}$_Thy_α-Tcp**) to 97.1% (**PVA$_{72000}$_PEBSA$_{25/75}$_Thy_α-Tcp**).

- *In vitro* cytotoxicity tests performed on the BALB/3T3 clone A31 cell line indicated the absence of cytotoxic effects of the antibacterial materials, with cell viability values exceeding 90% after 72 h of contact.
- The *in vivo* biocompatibility study, performed by subcutaneous implantation in Wistar rats, confirmed the biocompatibility of the tested materials, their integration with the host tissue, and the absence of an inflammatory response.
- The antibacterial hydrogels **PVA_{72000}_$PEBSA_{25/75}$_Thy_α-Tcp** contributed significantly to the reduction of wound size in Wistar rats. After 20 days of treatment, nearly complete wound healing (99.36%) was observed.

The obtained results support the potential of PVA_{72000}_$PEBSA_{25/75}$_Thy_α-Tcp systems for use in the development of wound dressings and tissue engineering applications.

Antibacterial hybrid hydrogels based on PVA_PEBSA_Dextran_Amx

- Three antibacterial double-network hybrid hydrogels based on PVA, PEBSA, dextran, and Amx were prepared using the freeze–thaw technique.
- FTIR spectra of the **PVA_{72000}_PEBSA_Dextran_Amx** systems highlighted the interactions between the blending components and the formation of intermolecular physical bonds.
- SEM images confirmed the encapsulation of Amx within the polymer matrix. This behavior was attributed to the hydrophobic affinity between the amphiphilic PEBSA copolymer and the antibiotic.
- *In vitro* enzymatic degradation tests demonstrated the resistance of the unloaded hydrogels to lipase action, as they were able to maintain the integrity of their polymer network for up to 28 days. A maximum mass loss ranging from 65% (**PVA_{72000}_$PEBSA_{50/50}$_Dextran**) to 70% (**PVA_{72000}_$PEBSA_{25/75}$_Dextran**) was recorded.
- Amx release from the **PVA_{72000}_PEBSA_Dextran_Amx** hybrid hydrogels exhibited an initial burst-release phase during the first 120–240 minutes, followed by a gradual release process that extended up to 94 h.
- The kinetic parameters of Amx release indicated a good fit of all systems to the Korsmeyer–Peppas model. The release exponent values for the **PVA_{72000}_$PEBSA_{25/75}$_Dextran_Amx** and **PVA_{72000}_$PEBSA_{75/25}$_Dextran_Amx**

systems suggested a predominantly Fickian release mechanism, in which the contribution of processes such as polymer erosion or relaxation is negligible. For the **PVA_{72000}_$PEBSA_{50/50}$_Dextran_Amx** sample, the data indicated a more complex release mechanism, in which diffusion is accompanied by structural changes within the polymer network associated with macromolecular chain relaxation.

- The **PVA_{72000}_PEBSA_Dextran_Amx** hybrid systems exhibited notable antibacterial activity against *E. coli*, with inhibition zone diameters ranging from 32.53 ± 2.71 mm (**PVA_{72000}_$PEBSA_{25/75}$_Dextran_Amx**) to 34.86 ± 2.65 mm (**PVA_{72000}_$PEBSA_{75/25}$_Dextran_ Amx**).
- Cytotoxicity assessments confirmed the cytocompatibility of the tested materials in contact with normal human dermal fibroblasts, without adverse effects on cell attachment or proliferation.
- The *in vitro* cell migration assay demonstrated the ability of the antibacterial hybrid hydrogels **PVA_{72000}_$PEBSA_{75/25}$_Dextran_Amx** to stimulate cell proliferation and migration, significantly reducing the time required for closure of the cell defect.

The obtained results confirm the potential of PVA_{72000}_$PEBSA_{75/25}$_Dextran_Amx hybrid hydrogels as efficient systems for the controlled release of bioactive substances, while also highlighting their promising applicability in tissue regeneration.

Antibacterial hybrid hydrogels based on PVA_PEBSA_Xanthan gum_Amx

- Three double-network hybrid hydrogels based on PVA_{72000} and PEBSA_Xanthan gum_Amx were prepared using the freeze–thaw technique.
- FTIR spectroscopy data confirmed the presence of antibacterial inclusions within the structure of the hybrid hydrogels, as well as the interactions between the components of the polymer networks.
- The microstructure of the **PVA_{72000}_PEBSA_Xanthan gum_Amx** hydrogels confirmed the presence of the antibiotic within the polymer matrix. Different forms of Amx microcrystals were observed, appearing as aggregates dispersed throughout the matrix.
- *In vitro* enzymatic degradation tests demonstrated good stability of the unloaded hydrogels against lipase action, with the materials maintaining their structural integrity for up to 28 days. Mass loss ranged from 43% (**PVA_{72000}_$PEBSA_{25/75}$_Xanthan gum**) to 62% (**PVA_{72000}_$PEBSA_{50/50}$_Xanthan gum**).

- The potential of the **PVA_{72000}_PEBSA_Xanthan gum** matrices to incorporate and release Amx through diffusion under *in vitro* conditions over a period of 94 h was demonstrated. The release profiles were best fitted by the Korsmeyer–Peppas kinetic model for the **PVA_{72000}_$PEBSA_{25/75}$_Xanthan gum_Amx** system and by the Higuchi model for the **PVA_{72000}_$PEBSA_{50/50}$_Xanthan gum_Amx** and **PVA_{72000}_$PEBSA_{75/25}$_Xanthan gum_Amx** systems.
- The **PVA_{72000}_PEBSA_Xanthan gum_Amx** hybrid systems exhibited a bacteriostatic effect against the growth of *S. aureus*, *E. coli*, and *K. pneumoniae*.
- *In vitro* cytotoxicity tests demonstrated the cytocompatibility of the tested materials toward normal human dermal fibroblasts, while the *in vitro* cell migration study highlighted the potential of the antibacterial hybrid hydrogels **PVA_{72000}_$PEBSA_{75/25}$_Xanthan gum_Amx** to promote the re-epithelialization process through the simultaneous stimulation of cell proliferation and migration.

The correlation of the obtained results supports the use of PVA_{72000}_$PEBSA_{75/25}$_Xanthan gum_Amx antibacterial hybrid hydrogels as efficient controlled drug delivery systems for tissue engineering applications, ensuring the prolonged availability of the bioactive substance over an extended period.

PERSPECTIVES

As a future perspective, the research and development directions initiated within this doctoral thesis will be further expanded and will focus on:

- simulation of the transdermal transport of bioactive substances using a vertical diffusion system with Franz cells, in order to characterize the release profile and permeability across the skin barrier;
- *in vivo* studies to evaluate the biocompatibility of the antibacterial hybrid hydrogels **PVA_{72000}_$PEBSA_{75/25}$_Dextran_Amx** and **PVA_{72000}_$PEBSA_{75/25}$_Xanthan gum_Amx**, through the assessment of local and systemic toxicity, inflammatory and immunological responses, tissue integration, as well as material degradation and resorption. These investigations will be conducted using animal experimental models, histopathological analyses of adjacent tissues, and biocompatibility tests, with the aim of validating the safety and efficacy of these materials for cutaneous wound healing;

- advanced studies on the antibacterial activity of **PVA_{72000}_$PEBSA_{25/75}$_Thy_α-Tcp** hydrogels using experimental infected wound models, with monitoring of the wound healing process, including inflammation remission and reduction of the time required for tissue regeneration.

SELECTIVE BIBLIOGRAPHY

[1] Zhao C, Zhou L, Chiao M, et al. Antibacterial hydrogel coating: Strategies in surface chemistry. Advances in Colloid and Interface Science 2020;285:102280. https://doi.org/10.1016/j.cis.2020.102280.

[2] Chen F-M, Liu X. Advancing biomaterials of human origin for tissue engineering. Progress in Polymer Science 2016;53:86–168. https://doi.org/10.1016/j.progpolymsci.2015.02.004.

[3] Kurakula M, Rao GK, Kiran V, et al. Alginate-based hydrogel systems for drug releasing in wound healing. Alginates in Drug Delivery, Elsevier; 2020, p. 323–58. https://doi.org/10.1016/B978-0-12-817640-5.00013-3.

[4] Xiong S, Li R, Ye S, et al. Vanillin enhances the antibacterial and antioxidant properties of polyvinyl alcohol-chitosan hydrogel dressings. International Journal of Biological Macromolecules 2022;220:109–16. https://doi.org/10.1016/j.ijbiomac.2022.08.052.

[5] Qi L, Zhang C, Wang B, et al. Progress in Hydrogels for Skin Wound Repair. Macromolecular Bioscience 2022;22:2100475. https://doi.org/10.1002/mabi.202100475.

[6] Adelnia H, Ensandoost R, Shebbrin Moonshi S, et al. Freeze/thawed polyvinyl alcohol hydrogels: Present, past and future. European Polymer Journal 2022;164:110974. https://doi.org/10.1016/j.eurpolymj.2021.110974.

[7] Plugariu I-A, Bercea M, Gradinaru LM, et al. Poly(vinyl alcohol)/Pullulan Composite Hydrogels as a Potential Platform for Wound Dressing Applications. Gels 2023;9:580. https://doi.org/10.3390/gels9070580.

[8] Bercea M. Recent Advances in Poly(vinyl alcohol)-Based Hydrogels. Polymers 2024;16:2021. https://doi.org/10.3390/polym16142021.

[9] Gonnet M, Lethuaut L, Boury F. New trends in encapsulation of liposoluble vitamins. Journal of Controlled Release 2010;146:276–90. https://doi.org/10.1016/j.jconrel.2010.01.037.

[19] González-Henríquez C, Sarabia-Vallejos M, Rodriguez-Hernandez J. Advances in the Fabrication of Antimicrobial Hydrogels for Biomedical Applications. Materials 2017;10:232. https://doi.org/10.3390/ma10030232.

[37] Fernández J, Amestoy H, Sardon H, et al. Effect of molecular weight on the physical properties of poly(ethylene brassylate) homopolymers. Journal of the Mechanical Behavior of Biomedical Materials 2016;64:209–19. https://doi.org/10.1016/j.jmbbm.2016.07.031.

[41] Slomkowski S, Basinska T, Gadzinowski M, et al. Polyesters and Polyester Nano- and Microcarriers for Drug Delivery. Polymers 2024;16:2503. https://doi.org/10.3390/polym16172503.

[42] Chiriac AP, Rusu AG, Nita LE, et al. Synthesis of Poly(Ethylene Brassylate-Co-squaric Acid) as Potential Essential Oil Carrier. Pharmaceutics 2021;13:477. https://doi.org/10.3390/pharmaceutics13040477.

[105] Ehterami A, Salehi M, Farzamfar S, et al. Chitosan/alginate hydrogels containing Alpha-tocopherol for wound healing in rat model. Journal of Drug Delivery Science and Technology 2019;51:204–13. https://doi.org/10.1016/j.jddst.2019.02.032.

[155] Pascual A, Sardon H, Veloso A, et al. Organocatalyzed Synthesis of Aliphatic Polyesters from Ethylene Brassylate: A Cheap and Renewable Macrolactone. ACS Macro Lett 2014;3:849–53. https://doi.org/10.1021/mz500401u.

[158] Pascual A, Sardón H, Ruipérez F, et al. Experimental and computational studies of ring-opening polymerization of ethylene brassylate macrolactone and copolymerization with ε-caprolactone and TBD-guanidine organic catalyst. J Polym Sci Part A: Polym Chem 2015;53:552–61. https://doi.org/10.1002/pola.27473.

[171] Stoica AE, Chircov C, Grumezescu AM. Hydrogel Dressings for the Treatment of Burn Wounds: An Up-To-Date Overview. Materials 2020;13:2853. https://doi.org/10.3390/ma13122853.

[186] **Crețu B-E-B**, Nita LE, Șerban A-M, et al. New Cryogels Based on Poly(vinyl alcohol) and a Copolymacrolactone System: I-Synthesis and Characterization. Nanomaterials 2022;12:2420. https://doi.org/10.3390/nano12142420.

[187] Nita LE, **Crețu B-E-B**, Șerban A-M, et al. New cryogels based on poly (vinyl alcohol) and a copolymacrolactone system. II. Antibacterial properties of the network embedded with thymol bioactive agent. Reactive and Functional Polymers 2023;182:105461. https://doi.org/10.1016/j.reactfunctpolym.2022.105461.

[195] **Crețu B-E-B**, Rusu AG, Ghilan A, et al. Cryogel System Based on Poly(vinyl Alcohol)/Poly(ethylene Brassylate-co-Squaric Acid) Platform with Dual Bioactive Activity. Gels 2023;9:174. https://doi.org/10.3390/gels9030174.

[220] Alves A, Miguel SP, Araujo ARTS, et al. Xanthan Gum–Konjac Glucomannan Blend Hydrogel for Wound Healing. Polymers 2020;12:99. https://doi.org/10.3390/polym12010099.

[211] **Crețu B-E-B**, Dodi G, Gardikiotis I, et al. Bioactive Composite Cryogels Based on Poly (Vinyl Alcohol) and a Polymacrolactone as Tissue Engineering Scaffolds: In Vitro and In Vivo Studies. Pharmaceutics 2023;15:2730. https://doi.org/10.3390/pharmaceutics15122730.

[223] Bernal-Chávez SA, Alcalá-Alcalá S, Tapia-Guerrero YS, et al. Cross-linked polyvinyl alcohol-xanthan gum hydrogel fabricated by freeze/thaw technique for potential application in soft tissue engineering. RSC Adv 2022;12:21713–24. https://doi.org/10.1039/D2RA02295H.

[224] Wang S, Wang Z, Xu C, et al. PEG- *α*- CD/AM/liposome @amoxicillin double network hydrogel wound dressing—Multiple barriers for long-term drug release. J Biomater Appl 2021;35:1085–95. https://doi.org/10.1177/0885328221991948.

APPENDIX 1. DISSEMINATION OF RESULTS AND SCIENTIFIC ACTIVITY

The original results obtained within the framework of this doctoral thesis have been disseminated through five published scientific articles, three oral communications, and three poster presentations:

Scientific articles published in ISI-indexed journals

1. **B.-E.-B. Crețu**, A.G. Rusu, D. Timpu, L.E. Nita. Sustainable pathways for poly(ethylene brassylate) synthesis. *Revue Roumaine de Chimie* **2025**, 70(7–8), 483–492, DOI: 10.33224/rrch.2025.70.7-8.12 (FI 0.6; Q4).
2. **B.-E.-B. Crețu**, G. Dodi, I. Gardikiotis, V. Balan, I. Nacu, I. Stoica, E. Stoleru, A.G. Rusu, A. Ghilan, L.E. Nita, A.P. Chiriac. Bioactive Composite Cryogels Based on Poly (Vinyl Alcohol) and a Polymacrolactone as Tissue Engineering Scaffolds: In Vitro and In Vivo Studies. *Pharmaceutics* **2023**, 15, 2730, https://doi.org/10.3390/pharmaceutics15122730 (FI 4.9; Q1).
3. **B.-E.-B. Crețu**, A.G. Rusu, A. Ghilan, I. Rosca, L.E. Nita, A.P. Chiriac. Cryogel System Based on Poly(vinyl alcohol)/Poly(ethylene brassylate-co-squaric acid) Platform with Dual Bioactive Activity. *Gels* **2023**, 9, 174, https://doi.org/10.3390/gels9030174 (FI 5.0; Q1).
4. L.E. Nita, **B.-E.-B. Crețu**, A.-M. Șerban, A.G. Rusu, I. Rosca, D. Pamfil, A.P. Chiriac. New Cryogels Based on Poly (Vinyl Alcohol) and a Copolymacrolactone System. II. Antibacterial Properties of the Network Embedded with Thymol Bioactive Agent. *Reactive and Functional Polymers* **2023**, 182, 105461, https://doi.org/10.1016/j.reactfunctpolym.2022.105461 (FI 4.5; Q1).
5. **B.-E.-B. Crețu**, L.E. Nita, A.-M. Serban, A.G. Rusu, F. Doroftei, A.P. Chiriac. New Cryogels Based on Poly(vinyl alcohol) and a Copolymacrolactone System: I-Synthesis and Characterization. *Nanomaterials* **2022**, 12, 2420, https://doi.org/10.3390/nano12142420 (FI 5.3; Q2).

Oral presentations at scientific conferences

1. Andrei-Alexandru IVU, **Bianca-Elena-Beatrice CRETU**, Alina Gabriela RUSU,

Loredana E. NITA, "*Ring-opening polymerization of renewable macrolactones for biodegradable polyester nanoparticles*", International Workshop on Multifunctional Polymer Composites for Advanced Applications, **March 26**, **2026**, Zabrze, Poland.

2. **Bianca-Elena-Beatrice Cretu**, Gianina Dodi, Ioannis Gardikiotis, Vera Balan, Alina Gabriela Rusu, Alina Ghilan, Loredana Elena Nita, Aurica P. Chiriac, "*Complex polymeric matrices with antibacterial and antioxidant inclusions*", Applications of Chemistry in Nanosciences and Biomaterials Engineering NanoBioMat 2024 – Summer Edition, **June 19-21**, **2024**.
3. **Bianca-Elena-Beatrice Cretu**, Alina G. Rusu, Mariana Cristea, Alina Ghilan, Loredana E. Nita, Aurica P. Chiriac, "*Cryogels based on poly(vinyl alcohol) and a copolymacrolactone system*", Spring School for Young Researchers „NEW TRENDS in EXPERIMENTAL MECHANICS – NTEM 1", **May 13–17**, **2024**, Zakopane, Poland.

Poster presentations

1. **Bianca-Elena-Beatrice Cretu**, Alina Gabriela Rusu, Loredana Elena Nita, "*Eco-friendly synthesis of poly(ethylene brassylate) as potential hydrophobic drug carrier*", International Congress of "Apollonia" University of Iași "Preparing the Future by Promoting Excellence", 35th Edition, **February 27–March 1**, **2025**, Iași, Romania.
2. **Bianca-Elena-Beatrice Cretu**, Vera Balan, Irina Rosca, Alexandru M. Serban, Alina Gabriela Rusu, Loredana Elena Nita, "*Hybrid cryogels as dermal drug delivery systems*", 5th Edition OPEN DOOR TO THE FUTURE – Scientific Communications of Young Researchers, MacroYouth 2024, **November 15**, **2024**, Iași, Romania.
3. **Bianca-Elena-Beatrice Crețu**, Alina Gabriela Rusu, Alina Ghilan, Isabella Nacu, Irina Rosca, Daniela Pamfil, Loredana Elena Nita, "*Poly(vinyl alcohol) and copolymacrolactone bioactive complex–based cryogels as promising wound dressings*", International Congress of "Apollonia" University of Iași "Preparing the Future by Promoting Excellence", 34th Edition, **February 29–March 3**, **2024**, Iași, Romania.

Scientific activity related to the topic of the doctoral thesis was materialized through three published scientific articles, one book currently under publication, one patent application, two oral communications, and five poster presentations:

Scientific articles published in ISI-indexed journals

1. S. Sandu, G. Dodi, I. Gardikiotis, **B.-E.-B. Cretu**, A. Luca, F. D. Cojocaru, L. Verestiuc, S.-A. Pasca, V. Balan. Co-encapsulated fluorescent magnetic nanoparticles for potential applications in breast cancer therapy: Exploratory in vitro and in vivo studies. *International Journal of Pharmaceutics* **2026**, 695, 126808, https://doi.org/10.1016/j.ijpharm.2026.126808 (FI 5.2; Q1).
2. A.G. Rusu, L.E. Niță, I. Roșca, A. Croitoriu, A. Ghilan, L. Mititelu-Tarțău, A.V. Grigoraș, **B.-E.-B. Crețu**, A.P. Chiriac. Alginate-Based Hydrogels Enriched with Lavender Essential Oil: Evaluation of Physicochemical Properties, Antimicrobial Activity, and In Vivo Biocompatibility. *Pharmaceutics* **2023**, 15, 2608, https://doi.org/10.3390/pharmaceutics15112608 (FI 4.9; Q1).
3. G. Dodi, R.E. Sabau, **B.E.-B. Crețu**, I. Gardikiotis. Exploring the Antioxidant Potential of Gellan and Guar Gums in Wound Healing. *Pharmaceutics* **2023**, 15, 2152, https://doi.org/10.3390/pharmaceutics15082152 (FI 4.9; Q1).

Book

1. Gianina Dodi, **Bianca-Elena-Beatrice Crețu**, Alexandra E. Avanu, "*Biocompatibility of Medical Devices: A Multidisciplinary Approach*", Editura "Gr. T. Popa", **2026** (in press).

Patent application

1. A.P. Chiriac, I. Neamțu, L.E. Niță, A.G. Rusu, A. Croitoriu, A.M. Șerban, **B.E.B. Crețu**, A. Ghilan, "*Procedeu de fabricare a unui hidrogel hibrid pe bază de polimer sintetic/agaroză*", A/00419/2023.

Oral presentations at scientific conferences

1. **B.-E.-B. Cretu**, K. Tadevosyan, A. Raya, G. Dodi, "*Magnetic nanosystems interactions*

with human induced pluripotent stem cells", COST Action CA17140 (NANO2CLINIC), 2nd CA17140 STSM Virtual Conference, **February 23**, **2023**.

2. V. Balan, S. Sandu, F.D. Cojocaru, A. Luca, G. Dodi, **B.E. Cretu**, L. Verestiuc, "*Co-encapsulated magnetic nanostructures based on functionalized chitosan for theranostic applications*", 9th International Conference „Biomaterials, Tissue Engineering & Medical Devices" BIOMMEDD'2022, **July 20–22**, **2022**, Bucharest, Romania.

Poster presentations

1. Alexandru-Mihail Serban, **Bianca-Elena-Beatrice Cretu**, Alina Gabriela Rusu, Alina Ghilan, Irina Rosca, Loredana Elena Nita, "*Development and characterization of levofloxacin-loaded vitamin A-polymacrolactone nanoemulsions as potential ophthalmic drug delivery systems*", International Congress of "Apollonia" University of Iași "Preparing the Future by Promoting Excellence", *35th Edition*, **February 27–March 1**, **2025**, Iași, Romania.
2. Vera Bălan, Ștefan Sandu, Vlad-Constantin Ursachi, **Bianca Elena Beatrice Crețu**, Florina Daniela Cojocaru, Gianina Dodi, Ioannis Gardikiotis, Andreea Luca, Liliana Vereștiuc, "*Biofunctionalized magnetic nanostructures based on biotinylated N-palmitoyl chitosan and magnetite for breast cancer applications: in vitro and in vivo studies*", 14th Romanian-Jordanian Congress of Medicine and Pharmacy (CORIMF 2024), **September 27–October 4**, **2024**, Iași, Romania.
3. Alina Gabriela Rusu, Aurica P. Chiriac, Loredana Elena Nita, Alina Ghilan, Alexandra Croitoriu, **Bianca Elena Beatrice Cretu**, Alexandru Mihail Serban, Alexandra Bargan, Florica Doroftei, "*Design of agarose-based aerogels with potential application as wound dressings*", COST Action CA18125 (AERoGELS), 3rd International Conference Aerogels for Biomedical and Environmental Applications, **July 5–7**, **2023**, Maribor, Slovenia.
4. G. Dodi, **B.E.B. Cretu**, F. Cojocaru, A.E. Avanu, I. Gardikiotis, "*Fabrication and evaluation of carboxymethyl guar gum based composites as wound healing dressings*", 30th Young Research Fellows Meeting (YRFM), **February 1–3**, **2023**, Paris, France.
5. V. Balan, V.C. Ursachi, F.D. Cojocaru, G. Dodi, C.T. Mihai, **B.E. Cretu**, L. Verestiuc, "*Design and preliminary in vitro evaluation of magnetic nanoparticles based on*

biotinylated N-palmitoyl chitosan for breast cancer applications", 19th International Conference on Nanosciences & Nanotechnologies (NN22), **July 5–8**, **2022**, Thessaloniki, Greece.

Research internship

1. Short-Term Scientific Mission (STSM) within COST Action CA18125 "Advanced Engineering and Research of aeroGels for Environment and Life Sciences (AERoGELS)", Institute of Chemical Sciences and Technologies "Giulio Natta", National Research Council (SCITEC-CNR), **October 9–14**, **2023**, Milan, Italy.

Attendance at thematic schools

1. Spring School for Young Researchers "NEW TRENDS in EXPERIMENTAL MECHANICS – NTEM 1", organized by the European Society for Experimental Mechanics (EURASEM) and the Institute of Fundamental Technological Research (IPPT PAN), **May 13–17**, **2024**, Zakopane, Poland.

Research projects

1. "Advanced and scalable multicomponent thermosensitive hydrogels for diabetic wound healing" – PN-IV-P7-7.1-PED-2024-1788.
2. "Hybrid bio-systems enriched with biotechnological extracted oils and applicability in skin tissue engineering" – PN-III-P2-2.1-PED-2021-2229.
3. "Co-encapsulated magnetic nanocarriers for theranostic applications in breast cancer: *in vivo* and *in vitro* studies" – PN-III-P1-1.1.-TE-2019-1671.